

Università degli Studi di Padova

DIPARTIMENTO DI MATEMATICA "TULLIO LEVI-CIVITA"

Corso di Laurea Magistrale in Matematica

TESI DI LAUREA MAGISTRALE

A Numerical Contribution to the Hierarchical Three-Body Problem

Candidato:

Edoardo Legnaro

Matricola 1149350

Relatore:

Gabriella Pinzari

Acknowledgements

I wish to express my deepest gratitude to my supervisor Prof. Gabriella Pinzari, for having followed and supported me step by step, with infinite patience, for having suggested the topic for this thesis and for having provided me with a draft version of her article [20], from which this thesis draws the foundations. Also, I would like to thank Prof. Massimiliano Guzzo for having suggested me how to proceed in implementing the code for the phase portraits of the second perturbation step on the two-centre Hamiltonian.

Contents

1	Introduction	7
2	The System	9
2.1	The Hierarchical Three-Body Problem	9
2.2	The Two-Centre Problem	12
2.3	Canonical Coordinates	13
3	The Unperturbed System	17
3.1	Two Perturbation Steps for Degenerate Systems	17
3.2	Numerical Results for the Unperturbed System	23
3.2.1	First Order Approximation	23
3.2.2	Second Order Approximation	26
3.3	The Full Planar Two-Centre Problem	29
4	The Full Perturbed System	35
4.1	Numerical Results	37
4.1.1	Collisions	38
	Appendices	51
A	Code	53
A.1	Unperturbed System	53
A.1.1	First Perturbation Step	53
A.1.2	Second Perturbation Step	54
A.2	The Perturbed System	56
A.2.1	Derivation of the Hamiltonian Vector Field	56
A.2.2	Spatial Positions of the Bodies	61
A.2.3	Numerical Solution of the Hamiltonian ODEs	62
A.3	Phase Portraits	66

Chapter 1

Introduction

The problem of studying the motion of mutually interacting celestial bodies has a very long tradition, and as always gripped human minds.

A big step forward in the comprehension of such problem is due to Isaac Newton, which solved in 1687 in [16] the two-body problem, consisting in determining the motion of two point particles that mutually interact through gravity. After this achievement, Newton also tackled in the same work the three body problem, in particular the one involving the Moon, the Earth and the Sun, but he couldn't manage to solve it.

The three-body problem became then a central topic in mathematical physics from the mid-1700s until the early 1900s. Various exact results were obtained for particular cases, but in the mid 1890's Henri Poincaré proved in [21] that the full three-body problem could not be solved in terms of algebraic formulas and integrals; in other words, he proved the non integrability of the three-body problem.

Also, his work laid the foundations for Hamiltonain Perturbation Theory, which in turn lead to KAM theory ([12], [14], [1]) and Nekhoroshev Theorem [15], thanks to which a major step forward in Celestial Mechanics had been done.

The two-centre problem consists of a single particle attracted by two fixed ones. Such problem was shown to be integrable by Euler in the 1760's ([7],[6]). Its solution is given in the form of a non-linear system involving elliptic integrals, as seen in [2]. A recent analysis of this problem have been performed in [22], [23] and [4]. It is also noteworthy the work of Ó'Mathúna, who devoted four chapters of his book [17] to the two-centre problem.

As presented in [19], it turns out that we can look at the hierarchical three body problem as a small perturbation of the two centre one.

It is precisely this point of view that constitutes the starting point of our

thesis, which finds its foundations in the two articles [19] and [20] and aims to provide a numerical investigation of the motions of the planar hierarchical three-body problem.

The structure of the thesis is as follows. We will first introduce in Chapter 2 the hierarchical three-body problem, following [19] and [20]. We will provide here an overview of the physical system and of its Hamiltonian, then we will introduce the two-centre problem and its Euler integral; finally at the end of the chapter we will recall a set of useful coordinates first introduced in [18] that will be used throughout our whole work.

In Chapter 3 we will analyse the planar two-centre problem. We will first find the second order normal form for degenerate systems, with all the details of the derivation. Next we will perform two perturbation steps on the Hamiltonian of the two-centre problem, providing phase portraits for both the first and the second order normal form. We will conclude comparing those with the phase portraits of the non-averaged Hamiltonian of the planar two-centre problem. Also, we will provide a detailed numerical analysis of a couple of particular orbits of this system.

Finally, in Chapter 4, we will report our numerical investigation of the planar hierarchical-tree body problem, providing a detailed analysis in some particular cases of the motion of all variables, as well as the spatial orbits of the three bodies. Here we also found that for some particular orbits the value of the Euler Integral stays almost constant for a finite time interval depending on the parameters and the initial point of the orbit, as can be seen in Figure 4.19.

Most of the code we have written and extensively used in our work is reported in Appendix.

Chapter 2

The System

In the following chapter we shall present the physical system we will be dealing with in this thesis.

2.1 The Hierarchical Three-Body Problem

The hierarchical three-body problem consists in tree point masses mutually interacting through gravity, with their masses in a hierarchical order. Namely, if we fix the largest mass m_1 , the mass of the second body is $m_2 = \mu m_1$ and the mass of the third one is $m_3 = \varepsilon \mu m_1$, where μ and ε are intended to be a couple of very small parameters, $\mu, \varepsilon \ll 1$. We will here provide a derivation of the hamiltonian of the system, following [19].

First of all we fix a orthonormal reference frame $(\mathbf{i}, \mathbf{j}, \mathbf{k})$ in \mathbb{R}^3 . Each mass m_i has a position vector \mathbf{q}_i and momentum¹ $\mathbf{p}_i = m_i \dot{\mathbf{q}}_i$.

This is an Hamiltonian problem, and the Hamiltonian is the following:²

$$H(\mathbf{p}, \mathbf{q}) = \sum_{i=1}^3 \frac{\|\mathbf{p}_i\|^2}{2m_i} - \sum_{1 \leq i < j \leq 3} \frac{m_i m_j}{\|\mathbf{q}_i - \mathbf{q}_j\|}, \quad (2.1)$$

where $\|\cdot\|$ denotes the usual Euclidian norm.

We now perform an *heliocentric reduction* in order to eliminate the motion of the most massive body. This is done by fixing the coordinates of the center of mass of the system \mathbf{Q} . The procedure is the following. Let \mathbf{P} be the total

¹We will indicate with a dot the time derivative $\frac{d}{dt}$

²It is the sum of the kinetic and of the potential energy, with gravitational constant set to one.

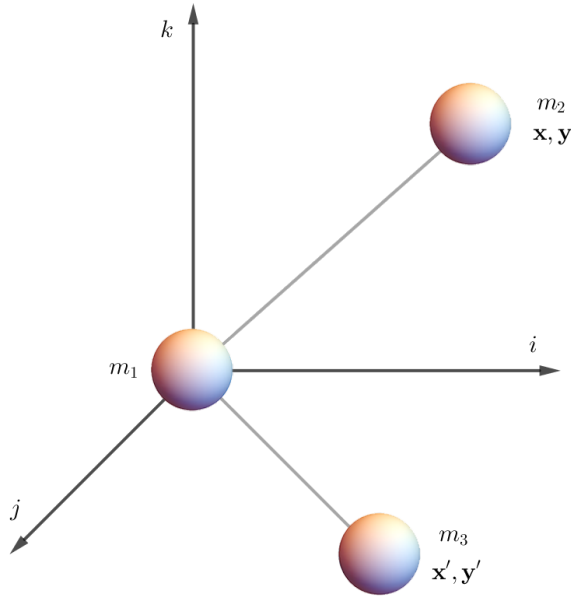


Figure 2.1: The hierarchical three-body system after the heliocentric reduction.

linear momentum: $\mathbf{P} = \sum_{i=1}^3 \mathbf{p}_i = \text{const } \dot{\mathbf{Q}}$, then consider the following change of variables

$$\begin{cases} \mathbf{x}_1 := \mathbf{q}_1 \\ \mathbf{x}_i := \mathbf{q}_i - \mathbf{q}_1 \quad i = 2, 3 \end{cases} \quad \begin{cases} \mathbf{y}_1 := \sum_{i=1}^3 \mathbf{p}_i = \mathbf{P} \\ \mathbf{y}_i := \mathbf{p}_i \quad i = 2, 3. \end{cases}$$

This change is a canonical transformation, since it is a linear one³. In this system the total linear momentum \mathbf{P} is a constant of motion, thus \mathbf{x}_1 is a cyclic variable, and, on the manifold where \mathbf{Q} is constant, we have $\mathbf{P} = 0$. So we can conveniently fix $\mathbf{x}_1 = 0$ and $\mathbf{P} = 0$, and now finding the reduced

³By canonical we mean, as usual, that the standard 2-form

$$\sum_{i=1}^3 \sum_{j=1}^3 dp_i \wedge dq_j$$

is preserved.

Hamiltonian amounts to substitute into (2.1)

$$\begin{cases} \mathbf{q}_1 = 0 \\ \mathbf{q}_i = \mathbf{x}_i & i = 2, 3 \end{cases} \quad \begin{cases} \mathbf{p}_1 := -\mathbf{p}_2 - \mathbf{p}_3 \\ \mathbf{p}_i := \mathbf{y}_i & i = 2, 3. \end{cases}$$

Consequently, (2.1) becomes

$$\tilde{H} = \frac{\|\mathbf{y}_2 + \mathbf{y}_3\|^2}{2m_1} + \frac{\|\mathbf{y}_2\|^2}{2m_2} + \frac{\|\mathbf{y}_3\|^2}{2m_3} - \frac{m_1 m_2}{\|\mathbf{x}_2\|} - \frac{m_1 m_3}{\|\mathbf{x}_3\|} - \frac{m_2 m_3}{\|\mathbf{x}_2 - \mathbf{x}_3\|}$$

but noticing that⁴ $\|\mathbf{y}_2 + \mathbf{y}_3\|^2 = (\mathbf{y}_2 + \mathbf{y}_3) \cdot (\mathbf{y}_2 + \mathbf{y}_3)$ we obtain that

$$\begin{aligned} \tilde{H} &= \frac{\|\mathbf{y}_2\|^2}{2} \left(\frac{m_1 + m_2}{m_1 m_2} \right) + \frac{\|\mathbf{y}_3\|^2}{2} \left(\frac{m_1 + m_3}{m_1 m_3} \right) \\ &\quad - \frac{m_1 m_2}{\|\mathbf{x}_2\|} - \frac{m_1 m_3}{\|\mathbf{x}_3\|} + \frac{\mathbf{y}_2 \cdot \mathbf{y}_3}{m_1} - \frac{m_2 m_3}{\|\mathbf{x}_2 - \mathbf{x}_3\|}, \end{aligned}$$

so defining

$$\begin{aligned} m' &= \frac{1}{\mu} \frac{m_1 m_2}{m_1 + m_2} = \frac{m_1}{1 + \mu}, & m &= \frac{1}{\varepsilon \mu} \frac{m_1 m_3}{m_1 + m_3} = \frac{m_1}{1 + \varepsilon \mu}, \\ M' &= m_1(1 + \mu), & M &= m_1(1 + \varepsilon \mu), \end{aligned}$$

and

$$\mathbf{x}_2 = \mathbf{y}', \quad \mathbf{x}_3 = y, \quad \mathbf{y}_2 = \mathbf{y}', \quad \mathbf{y}_3 = \mathbf{y}$$

and noticing that $m_2 m_3 = \varepsilon \mu^2 m_1^2 = \varepsilon \mu^2 m M$, we find that

$$\tilde{H}(\mathbf{X}, \mathbf{Y}) = \frac{\|\mathbf{y}'\|^2}{2\mu m'} - \frac{\mu m' M'}{\|\mathbf{x}'\|} + \frac{\|\mathbf{y}\|^2}{2\varepsilon \mu m} - \frac{\varepsilon \mu m M}{\|\mathbf{x}\|} + \frac{\mathbf{y}' \cdot \mathbf{y}}{m_1} - \frac{\varepsilon \mu^2 m M}{\|\mathbf{x} - \mathbf{x}'\|}, \quad (2.2)$$

where $\mathbf{X} = (\mathbf{x}', \mathbf{x})$ and $\mathbf{Y} = (\mathbf{y}', \mathbf{y})$.

We can still make another simplification by rescaling time and impulses as

$$t = \mu \bar{t}, \quad \mathbf{Y} = \varepsilon \mu \bar{\mathbf{Y}},$$

so that the new Hamiltonian becomes

$$\bar{H}(\bar{\mathbf{X}}, \bar{\mathbf{Y}}) := \frac{1}{\mu} \tilde{H}(\mathbf{X}, \varepsilon \mu \bar{\mathbf{Y}}).$$

⁴We will denote with \cdot the scalar product.

Then, neglecting the "bars", we find that the Hamiltonian of the system can be written in the following form:

$$H(\mathbf{X}, \mathbf{Y}) = -\frac{m'M'}{\|\mathbf{x}'\|} + \varepsilon \left(\frac{\|\mathbf{y}\|^2}{2m} - \frac{mM}{\|\mathbf{x}\|} - \frac{\mu m M}{\|\mathbf{x} - \mathbf{x}'\|} \right) \quad (2.3)$$

$$+ \varepsilon^2 \left(\frac{\|\mathbf{y}'\|^2}{2m'} + \frac{\mu}{m_1} \mathbf{y}' \cdot \mathbf{y} \right). \quad (2.4)$$

We define

$$h_0(\mathbf{x}') := -\frac{m'M'}{\|\mathbf{x}'\|},$$

$$h_1(\mathbf{y}, \mathbf{x}', \mathbf{x}) := \frac{\|\mathbf{y}\|^2}{2m} - \frac{mM}{\|\mathbf{x}\|} - \frac{\mu m M}{\|\mathbf{x} - \mathbf{x}'\|},$$

$$f(\mathbf{y}, \mathbf{y}') := \frac{\|\mathbf{y}'\|^2}{2m'} + \frac{\mu}{m_1} \mathbf{y}' \cdot \mathbf{y},$$

so that we can write H as

$$H = h_0 + \varepsilon h_1 + \varepsilon^2 f.$$

2.2 The Two-Centre Problem

Notice that the Hamiltonian h_1 is the Hamiltonian of the *two-centre problem*, which is the problem of determining the motions of one moving mass in the gravitational field generated by two fixed masses. In our case, the moving mass is m and the two fixed ones are M and μM , which are posed, respectively, at the origin and at \mathbf{x}' . So this system is a good initial approximation for the three-body one.

From a purely mathematical point of view, the two-centre problem is very interesting, since it belongs to the the very restrictive class of Liouville-integrable dynamical systems. Its resolvability was first established by Euler in the 1760's in [7, 6].

As done in [20, 19], for our aims it will be convenient to regard h_1 as a *six degrees of freedom system*, i.e. as a function of

$$\mathbf{y}', \mathbf{y} \in \mathbb{R}^3, \quad \mathbf{x}' \in \mathbb{R}^3 \setminus \{0\}, \quad \mathbf{x} \in \mathbb{R}^3 \setminus \{0, \mathbf{x}'\}.$$

We define the angular momentum of the second and of the third body respectively as $\mathbf{C}' = \mathbf{x}' \times \mathbf{y}'$ and $\mathbf{C} = \mathbf{x} \times \mathbf{y}$. In the enlarged phase space the

vectors \mathbf{x}' and $\mathbf{C}_{\text{tot}} = \mathbf{C} + \mathbf{C}'$ (the total angular momentum vector) are first integrals to h_1 . We then have *six* conserved quantities, which however are not mutually in involution. It is anyway possible to extract out of such six quantities, the following four commuting ones:

$$Z := \mathbf{C}_{\text{tot}} \cdot \mathbf{k}, \quad C := \|\mathbf{C}_{\text{tot}}\|, \quad \Theta := \frac{\mathbf{C} \cdot \mathbf{x}'}{\|\mathbf{x}'\|}, \quad r' := \|\mathbf{x}'\|. \quad (2.5)$$

Besides these, the integrability of h_1 relies on the existence of a further independent commuting first integral J , found by Euler and hence called *Euler's integral*.

It is defined as follows. Notice first of all that h_1 can be written as⁵ $h_1 = h_{\text{kep}} + \mu g$, with

$$h_{\text{kep}} = \frac{\|\mathbf{y}\|^2}{2m} - \frac{mM}{\|\mathbf{x}\|}, \quad g = -\frac{mM}{\|\mathbf{x} - \mathbf{x}'\|}.$$

Then, J is defined by

$$J = J_0 + \mu J_1, \quad (2.6)$$

with

$$J_0 := \|C\|^2 - \mathbf{x}' \cdot \mathbf{L}, \quad J_1 := m^2 M \frac{(\mathbf{x}' - \mathbf{x}) \cdot \mathbf{x}'}{\|\mathbf{x}' - \mathbf{x}\|},$$

where \mathbf{L} is the *Lenz vector* associated to h_{kep} :

$$\mathbf{L} := \mathbf{y} \times \mathbf{C} - m^2 M \frac{\mathbf{x}}{\|\mathbf{x}\|}.$$

A derivation of J can be found in [20, 19].

2.3 Canonical Coordinates

We will use in the rest of this thesis the set of canonical coordinates first introduced in [18]

$$\mathbf{k} = ((Z, C, \Theta, G, \Lambda), (z, \gamma, g, \ell), (R', r')), \quad (2.7)$$

as are defined in [20].

⁵Here h_{kep} is the Hamiltonian which describes the keplerian orbits of the body of mass m around a fixed one of mass M . Notice that h_1 reduces to h_{kep} when $\mathbf{x} = \mathbf{x}'$

As seen in [20], the Hamiltonian (2.3) and the first integral J in (2.6) in the planar case becomes

$$H = -\frac{m'M'}{r'} + \varepsilon E + \varepsilon^2 f \quad (2.8)$$

where

$$E = -\frac{m^3 M^2}{2\Lambda^2} - \mu \frac{mM}{\sqrt{r'^2 + 2r'a\varrho \cos(g + \nu) + a^2\varrho^2}} \quad (2.9)$$

$$f = \frac{R'^2}{2m'} + \frac{(C - G)^2}{2r'^2 m'} + \frac{\mu}{m_1} \mathbf{y}'_k \cdot \mathbf{y}_k \quad (2.10)$$

with

$$\begin{aligned} \mathbf{y}' \cdot \mathbf{y} = & -\frac{1}{\Lambda r(e \cos \zeta - 1)} \left(m^2 M \left(\sin g \left(rR \cos \zeta \frac{G}{\Lambda} - \sin \zeta (G + C) \right) + \right. \right. \\ & \left. \left. + \cos g \left(\cos \zeta \frac{G}{\Lambda} (G + C) + rR \sin \zeta \right) \right) \right) \end{aligned}$$

and

$$J = J_0 + \mu J_1, \quad (2.11)$$

where

$$\begin{aligned} J_0 &= G^2 + m^2 M r' \sqrt{1 - \frac{G^2}{\Lambda^2}} \cos g \\ J_1 &= m^2 M r' \frac{r' + a\varrho \sqrt{1 - \frac{\Theta^2}{G^2}} \cos(g + \nu)}{\sqrt{r'^2 + 2r'a\varrho \cos(g + \nu) + a^2\varrho^2}}. \end{aligned}$$

We also report the formulae that expresses $(\mathbf{x}, \mathbf{x}', \mathbf{y}, \mathbf{y}')$ as a function of the variables k : if we define

$$R_1(\alpha) := \begin{pmatrix} 1 & 0 & 0 \\ 0 & \cos \alpha & -\sin \alpha \\ 0 & \sin \alpha & \cos \alpha \end{pmatrix}$$

$$R_3(\alpha) := \begin{pmatrix} \cos \alpha & -\sin \alpha & 0 \\ \sin \alpha & \cos \alpha & 0 \\ 0 & 0 & 1 \end{pmatrix}$$

$$\mathbf{e}_3 := \begin{pmatrix} 0 \\ 0 \\ 1 \end{pmatrix}.$$

then it holds

$$\begin{cases} \mathbf{x} = R_3(z)R_1(\iota)R_3(\gamma)R_1(\iota_1)R_3(\theta)R_1(\iota_2)\mathbf{x}_{d,pl} \\ \mathbf{y} = R_3(z)R_1(\iota)R_3(\gamma)R_1(\iota_1)R_3(\theta)R_1(\iota_2)\mathbf{y}_{d,pl} \\ \mathbf{x}' = \mathbf{r}'R_3(z)R_1(\iota)R_3(\gamma)R_1(\iota_1)\mathbf{k} \\ \mathbf{y}' = \frac{\mathbf{R}'}{\mathbf{r}'}\mathbf{x}'_k + \frac{1}{\mathbf{r}'^2}\mathbf{C}' \times \mathbf{x}' \end{cases} \quad (2.12)$$

with

$$\mathbf{x}_{d,pl} = \frac{\Lambda^2}{m^2 M} \begin{pmatrix} \cos \zeta - e \\ \sqrt{1-e^2} \sin \zeta \\ 0 \end{pmatrix} \quad (2.13)$$

$$\mathbf{y}_{d,pl} = \frac{m^2 M}{\Lambda \varrho} R_3(g - \frac{\pi}{2}) \begin{pmatrix} -\sin \zeta \\ \sqrt{1-e^2} \cos \zeta \\ 0 \end{pmatrix} \quad (2.14)$$

$$\mathbf{C}_{tot} = C R_3(z)R_1(\iota)\mathbf{e}_3 \quad (2.15)$$

$$\mathbf{C} = G R_3(z)R_1(\iota)R_3(\gamma)R_1(\iota_1)R_3(\theta)R_1(\iota_2)\mathbf{e}_3 \quad (2.16)$$

$$\mathbf{C}' = \mathbf{C}_{tot} - \mathbf{C} = R_3(z)R_1(\iota) (C\mathbb{I} - G R_3(\gamma)R_1(\iota_1)R_3(\theta)R_1(\iota_2)) \mathbf{e}_3, \quad (2.17)$$

where, if

$$e = e(\Lambda, G) = \sqrt{1 - \frac{G^2}{\Lambda^2}}$$

is the eccentricity, then $\zeta = \zeta(\Lambda, G, \ell)$ is the *eccentric anomaly*, defined as the unique solution of the *Kepler equation*

$$\ell = \zeta - e(\Lambda, G) \sin \zeta,$$

moreover

$$\varrho = \varrho(\Lambda, G, \ell) := 1 - e \cos \zeta,$$

and finally $\nu = \nu(\Lambda, G, \ell)$ is the *true anomaly*, defined by

$$\nu = \arg \left(\cos \zeta - e, \frac{G}{\Lambda} \sin \zeta \right).$$

Chapter 3

The Unperturbed System

We now start our analysis from the unperturbed system in the planar case, which is the two-body one with Hamiltonian E in (2.9). On such Hamiltonian, we will perform two perturbation steps in order to get a first approximation of the motion. We will first outline the general theory for a generic degenerate Hamiltonian system, then we shall provide the results for the Hamiltonian E . For an account on degenerate systems we refer to [9] and [10].

3.1 Two Perturbation Steps for Degenerate Systems

Consider a degenerate Hamiltonian system, with Hamiltonian in action-angle coordinates

$$H(I, \varphi, u, v) = h(I) + \mu f(I, \varphi, u, v), \quad (3.1)$$

where μ is a small parameter. We aim to find a near the identity canonical transformation¹ that puts H in a form independent of the angle φ up to the order μ^2 . We will do so by using the so called *Lie Series* method, which consists in constructing the canonical transformation as the time μ map of a generating hamiltonian. You can find a general account of this method in [3],[8] and in [13], where is also considered the degenerate case.

¹Namely, such that the new variables $\tilde{I}, \tilde{\varphi}, \tilde{u}, \tilde{v}$ satisfies

$$\tilde{I} = I + \mu \dots, \quad \tilde{\varphi} = \varphi + \mu \dots, \quad \tilde{u} = u + \mu \dots, \quad \tilde{v} = v + \mu \dots$$

Notations

We will first fix some notations. Given any two functions F, G of (I, φ, u, v) , we shall denote as ∇F the gradient and with \mathbb{E} the *symplectic identity*:

$$\mathbb{E} = \begin{pmatrix} 0 & -\mathbb{I} \\ \mathbb{I} & 0 \end{pmatrix}.$$

We will write their *Poisson bracket* as

$$\begin{aligned} \{F, G\} &= \nabla F \cdot \mathbb{E} \nabla G = \{F, G\}_{I,\varphi} + \{F, G\}_{u,v} = \\ &= \frac{\partial f}{\partial I} \frac{\partial g}{\partial \varphi} - \frac{\partial f}{\partial \varphi} \frac{\partial g}{\partial I} + \frac{\partial f}{\partial u} \frac{\partial g}{\partial v} - \frac{\partial f}{\partial v} \frac{\partial g}{\partial u}. \end{aligned}$$

We will also write ∂_I for $\frac{\partial}{\partial I}$, and similarly for the other variables. Given a vector field X , we shall denote the *Lie derivative* associated to X as L_X , and as ϕ_X^t the time t flow of X . In the case of an Hamiltonian vector field X_H associated to an Hamiltonian H , we will write for shortness L_H and ϕ_H^t . It holds for every F, G

$$F \circ \phi_G^s = e^{sL_G} F = \sum_{k=0}^{\infty} \frac{s^k}{k!} L_G^k F.$$

Moreover, for any function $F(I, \varphi, u, v)$, we will write $\bar{F}(I, u, v)$ or $\langle F \rangle$ for the average over the angle φ :

$$\bar{F} = \frac{1}{2\pi} \int_0^{2\pi} F(I, \varphi, u, v) d\varphi,$$

and we define $\tilde{F} = F - \bar{F}$.

For the Hamiltonian $h(I)$ in (3.1) we define

$$\omega(I) := \frac{\partial h}{\partial I}(I).$$

Second-Order Normal Form

We will now prove the following

Theorem 1. *Consider a degenerate Hamiltonian system with Hamiltonian in action angle coordinates as in (3.1). Then there exists two generating Hamiltonians χ_1, χ_2 such that*

$$H \circ \phi_{\chi_1}^\mu \circ \phi_{\chi_2}^{\mu^2} = h(I) + \mu \bar{f}(I, u, v) + \mu^2 (f_{21} + f_{22})(I, u, v) + \mathcal{O}(\mu^3),$$

with

$$\begin{aligned} f_{21}(I, u, v) &= -\frac{1}{4\pi} \partial_I \int_0^{2\pi} \frac{1}{\omega} (f^2 - \bar{f}) d\varphi, \\ f_{22}(I, u, v) &= \frac{1}{\omega} \left(-\frac{1}{4\pi^2} \int_0^{2\pi} d\varphi \int_0^\varphi d\psi \int_0^{2\pi} d\alpha \partial_u f(\alpha) \partial_v f(\alpha - \psi) + \right. \\ &\quad \left. \frac{1}{4\pi} \int_0^{2\pi} d\psi \int_0^{2\pi} d\alpha \partial_u f(\alpha) \partial_v f(\alpha - \psi) \right). \end{aligned}$$

Proof. It holds

$$\begin{aligned} H \circ \phi_{\chi_1}^\mu &= \sum_{k=0}^{\infty} \frac{\mu^k}{k!} L_{\chi_1}^k H \\ h + \mu \left(f + L_{\chi_1} h \right) + \mu^2 \left(L_{\chi_1} f + \frac{1}{2} L_{\chi_1}^2 h \right). \end{aligned}$$

We impose the term of μ order to be independent of the angle φ , so we must chose χ_1 so that $f + L_{\chi_1} h = g(I, u, v)$, but then taking the average over φ on both terms yields

$$f + L_{\chi_1} h = \bar{f}.$$

Notice that this also gives us

$$L_{\chi_1} h = -\tilde{f} \implies L_{\chi_1}^2 h = -L_{\chi_1} \tilde{f}.$$

We could find an analytical expression for χ_1 by writing it and the perturbation in Fourier series expansion: since it holds

$$L_{\chi_1} h = \{h, \chi_1\} = \omega \frac{\partial \chi_1}{\partial \varphi}$$

we find the *homological equation*

$$\omega \frac{\partial \chi_1}{\partial \varphi} = -f + \bar{f}, \tag{3.2}$$

and so if we expand in Fourier series $\chi_1 = \sum_k \hat{\chi}_k(I, u, v) e^{ik\varphi}$ and $\bar{f} - f = \sum_{k \neq 0} \hat{f}_k(I, u, v) e^{ik\varphi}$ we get from (3.2)

$$\sum_k ik \hat{\chi}_k e^{ik\varphi} = -\frac{1}{\omega} \sum_{k \neq 0} \hat{f}_k e^{ik\varphi}.$$

The harmonic $\hat{\chi}_0$ (which is equal to the φ -average of χ_1) remains free, thus we can choose it to be zero. Finally we find that χ_1 can be written as

$$\chi_1(I, \varphi, u, v) = - \sum_{k \neq 0} \frac{\hat{f}_k}{ik\omega} e^{ik\varphi}.$$

So at the first perturbation step we have

$$H \circ \phi_{\chi_1}^\mu = h(I) + \mu \bar{f} + \mu^2 \left(L_{\chi_1} f + \frac{1}{2} L_{\chi_1}^2 h \right). \quad (3.3)$$

Moving on to the second perturbation step, it holds

$$\begin{aligned} H \circ \phi_{\chi_1}^\mu \circ \phi_{\chi_2}^{\mu^2} &= \sum_{k=0}^{\infty} \frac{\mu^{2k}}{k!} L_{\chi_2}^k (H \circ \phi_{\chi_2}^\mu) = \\ &= h + \mu \bar{f} + \mu^2 \left(L_{\chi_1} f + L_{\chi_2} h + \frac{1}{2} L_{\chi_1}^2 h \right) + \mathcal{O}(\mu^3). \end{aligned}$$

The μ^2 order term must become independent of the angle φ , so similarly to before we must chose χ_2 in order to have²

$$\begin{aligned} L_{\chi_1} f + L_{\chi_2} h + \frac{1}{2} L_{\chi_1}^2 h &= \langle L_{\chi_1} f \rangle + \langle L_{\chi_1}^2 h \rangle = \\ &\stackrel{f=\tilde{f}-\bar{f}}{=} \langle L_{\chi_1} \tilde{f} \rangle - \frac{1}{2} \langle L_{\chi_1}^2 h \rangle = \\ &= \frac{1}{2} \langle L_{\chi_1}^2 \tilde{f} \rangle. \end{aligned}$$

But

$$\langle L_{\chi_1}^2 \tilde{f} \rangle = \langle \{\tilde{f}, \chi_1\} \rangle = \langle \{\tilde{f}, \chi_1\} \rangle_{I, \varphi} + \langle \{\tilde{f}, \chi_1\} \rangle_{u, v},$$

so next we will write more explicitly the two terms on the left hand side, and this will bring us to f_{21} and f_{22} as written in the statement. We begin with

²We recall that the derivative with respect to an angle of a periodic function must have null mean, so we have $\langle L_{\chi_2} h \rangle = 0$.

the first term: it holds

$$\begin{aligned}
 \frac{1}{2} \langle \{\tilde{f}, \chi_1\}_{I,\varphi} \rangle &= \frac{1}{2} \left\{ \sum_{\ell,k \neq 0} \left\langle \hat{f}_k e^{ik\varphi}, -\frac{\hat{f}_\ell}{i\ell\omega} e^{il\varphi} \right\rangle \right\} = \\
 &= \frac{1}{2} \left\langle \sum_{\ell,k \neq 0} \left(-\partial_I \hat{f}_k \cdot \frac{\hat{f}_\ell}{i\ell\omega} \mathcal{M} + ik \hat{f}_k \partial_I \frac{\hat{f}_\ell}{i\ell\omega} \right) e^{i(\ell+k)\omega} \right\rangle = \\
 &\stackrel{*}{=} -\frac{1}{2} \sum_{k \neq 0} \left(\partial_I \hat{f}_k \cdot \frac{\hat{f}_{-k}}{\omega} + \hat{f}_k \cdot \partial_I \frac{\hat{f}_{-k}}{\omega} \right) = \\
 &= -\frac{1}{2} \sum_{k \neq 0} \partial_I \left(\hat{f}_k \cdot \frac{\hat{f}_{-k}}{\omega} \right) = -\frac{1}{2} \partial_I \frac{1}{\omega} \sum_{k \neq 0} \hat{f}_k \hat{f}_{-k} = \\
 &\stackrel{\circledast}{=} -\frac{1}{4\pi} \partial_I \int_0^{2\pi} \frac{1}{\omega} (f^2 - \bar{f}^2) d\varphi,
 \end{aligned}$$

And we have thus found f_{21} . We used in \circledast the fact that taking the average is corresponds to taking $k = -\ell$ and in \circledast the *Parseval identity*:

$$\frac{1}{2\pi} \int_0^{2\pi} f^2 d\varphi = \sum_{k \neq 0} \hat{f}_k \hat{f}_{-k} + \bar{f}^2.$$

We now move on to the second term: it holds

$$\begin{aligned}
 \frac{1}{2} \langle \{\tilde{f}, \chi_1\}_{u,v} \rangle &= \frac{1}{2} \left\langle \sum_{k \neq 0} \sum_{\ell \neq 0} \left\{ \frac{\hat{f}_k}{ik\omega}, \hat{f}_\ell \right\}_{u,v} e^{i(k+\ell)\varphi} \right\rangle = \\
 &= \frac{1}{2} \sum_{k \neq 0} \left\{ \frac{\hat{f}_k}{ik\omega}, \hat{f}_{-k} \right\}_{u,v} = \frac{1}{2} \sum_{k \neq 0} \frac{1}{ik\omega} \left(\partial_u \hat{f}_k \partial_v \hat{f}_{-k} \partial_v \hat{f}_k \partial_u \hat{f}_{-k} \right) = \\
 &= \sum_{k \neq 0} \frac{1}{ik\omega} \partial_u \hat{f}_k \partial_v \hat{f}_{-k}.
 \end{aligned}$$

We then define the following "convolution" product for any function F, G

$$(F * G)(\varphi) := \frac{1}{2\pi} \int_0^{2\pi} F(\psi) G(\psi - \varphi) d\psi.$$

If we can expand F and G in Fourier series $F(\varphi) = \sum_k \hat{F}_k e^{ik\varphi}$, $G(\varphi) = \sum_k \hat{G}_k e^{ik\varphi}$, then

$$\begin{aligned} (F * G)(\varphi) &= \frac{1}{2\pi} \int_0^{2\pi} \sum_{k,\ell} \hat{F}_k \hat{G}_\ell e^{ik\psi} e^{i\ell(\psi-\varphi)} d\psi = \\ &= \sum_k \hat{F}_k \hat{G}_{-k} e^{ik\varphi}, \end{aligned}$$

so $\hat{F}_k \hat{G}_{-k}$ are the Fourier coefficients of $F * G$. For another generic function $K = \sum_{j \neq 0} \hat{K}_j e^{ij\varphi}$ with null mean, it holds

$$\begin{aligned} \sum_{j \neq 0} \frac{\hat{K}_j}{ij} e^{ij\varphi} &= \text{primitive of } K \text{ with null mean} = \\ &= \int_0^\varphi K(\psi) d\psi - \frac{1}{2\pi} \int_0^{2\pi} \left(\int_0^\varphi K(\psi) d\psi \right) d\varphi, \end{aligned}$$

so for $\varphi = 0$ we get

$$\sum_{j \neq 0} \frac{\hat{K}_j}{ij} = -\frac{1}{2\pi} \int_0^{2\pi} \left(\int_0^\varphi K(\psi) d\psi \right) d\varphi.$$

Taking $K = F * G - \langle F * G \rangle = \sum_{k \neq 0} \hat{F}_k \hat{G}_{-k} e^{ik\varphi}$ yields

$$\begin{aligned} \sum_{k \neq 0} \frac{\hat{F}_k \hat{G}_{-k}}{ik\omega} &= -\frac{1}{2\pi} \int_0^{2\pi} \left(\int_0^\varphi (F * G)(\psi) - \langle F * G \rangle d\psi \right) d\varphi = \\ &= \frac{1}{\omega} \left(-\frac{1}{4\pi^2} \int_0^{2\pi} d\varphi \int_0^\varphi d\psi \int_0^{2\pi} d\alpha F(\alpha) G(\alpha - \psi) + \right. \\ &\quad \left. + \frac{1}{4\pi} \int_0^{2\pi} d\psi \int_0^{2\pi} d\alpha F(\alpha) G(\alpha - \psi) \right), \end{aligned}$$

so finally if we take $F = \partial_u f$ and $G = \partial_v f$ we that $\frac{1}{2} \langle \{\tilde{f}, \chi_1\}_{u,v} \rangle$ is equal to f_{22} in the statement, and this ends the proof. \square

3.2 Numerical Results for the Unperturbed System

3.2.1 First Order Approximation

Lets come back to the Hamiltonian

$$E = -\frac{m^3 M^2}{2\Lambda^2} - \mu \frac{mM}{\sqrt{r'^2 + 2r'a\varrho \cos(g+\nu) + a^2\varrho^2}},$$

which is the one of the two-body problem written in the aforementioned k-coordinates. If we collect inside the square root the term a^2 , recalling that $\delta = \frac{r'}{a}$, we get

$$\begin{aligned} E &= -\frac{m^3 M^2}{2\Lambda^2} - \mu \frac{mM}{a\sqrt{\delta^2 + 2\delta\varrho \cos(g+\nu) + \varrho^2}} = \\ &= \frac{r'}{\mu m M} \left(-\frac{\mu m M}{r'} \frac{m^3 M^2}{2\Lambda^2} - \frac{\delta}{\sqrt{\delta^2 + 2\delta\varrho \cos(g+\nu) + \varrho^2}} \right). \end{aligned}$$

Now, it is possible to reabsorb the multiplicative constant with a rescaling of time. Also, since R' nor ℓ are present in the Hamiltonian E , the term $-\frac{\mu m M}{r'} \frac{m^3 M^2}{2\Lambda^2}$ will stay constant, and thus we will neglect it. We will consider the rescaled variable $\widehat{G} := \frac{G}{\Lambda}$, and we will study the motion of the system averaged over the "secular" variable ℓ , in order to provide a first approximation of the motion of the system in the plane (g, \widehat{G}) .

It will be useful to work with the eccentric anomaly ζ instead of the mean anomaly ℓ . So, recalling the relations

$$\begin{aligned} \ell &= \zeta - e \sin \zeta, & \varrho &= 1 - e \cos \zeta, \\ \cos \nu &= \frac{\cos \zeta - e}{1 - e \cos \zeta}, & \sin \nu &= \frac{\sqrt{1 - e^2} \sin \zeta}{1 - e \cos \zeta}, \end{aligned} \quad (3.4)$$

we have that the average of

$$U := -\frac{\delta}{\sqrt{\delta^2 + 2\delta\varrho \cos(g+\nu) + \varrho^2}}$$

can be written as

$$\begin{aligned} \bar{U} &= \frac{1}{2\pi} \int_0^{2\pi} U d\ell = -\frac{\delta}{2\pi} \int_0^{2\pi} (1 - e \cos \zeta) \cdot \\ &\quad \cdot \frac{1}{\sqrt{\delta^2 + 2\delta(\cos g(\cos \zeta - e) - \sqrt{1 - e^2} \sin g \sin \zeta) + (1 - e \cos \zeta)^2}} d\zeta. \end{aligned}$$

So, since at first order the approximation of the Hamiltonian is given by its mean over the angle ℓ , as seen in 1, we can thus get a first approximation of the motion by plotting the level sets of \bar{U} , and we get the pictures collected in 3.2.1. We remark that in such graphics it is not shown the separatrix, namely the level set through $(0, 0)$, since for the points in it the denominator of U goes to zero, and so we cannot see properly this level set numerically.

The Matlab code used in order to get such graphics is reported in A.1.1

Level sets of \bar{U}

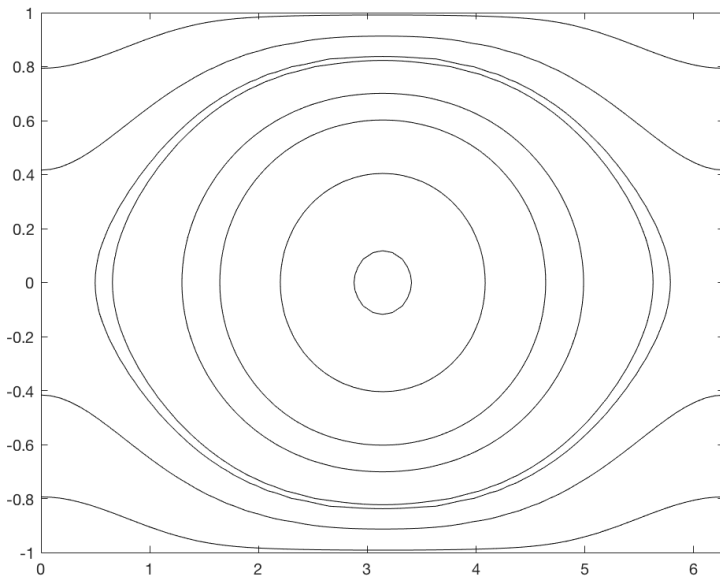


Figure 3.1: Case $\delta \in (0, 1)$, here it is shown the particular case $\delta = \frac{1}{2}$.

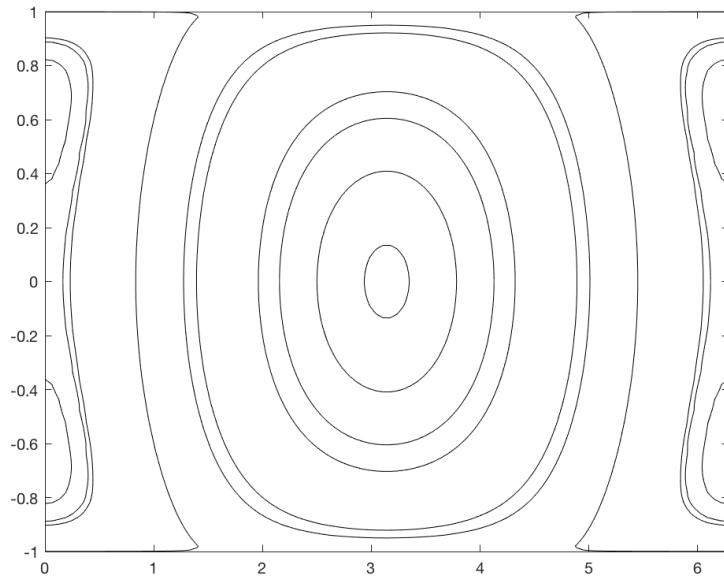


Figure 3.2: Case $\delta \in (1, 2)$, here it is shown the particular case $\delta = \frac{3}{2}$.

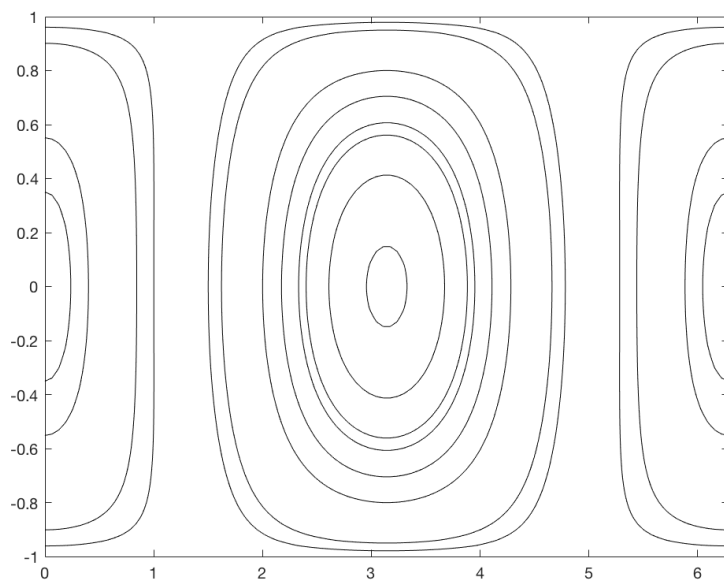


Figure 3.3: Case $\delta > 2$, here it is shown the particular case $\delta = \frac{5}{2}$.

3.2.2 Second Order Approximation

We now move on to the second order approximation. Here we cannot make the same simplification that we have done at the first order by gathering some constants. We will thus consider the Hamiltonian (cfr. Theorem 1)

$$H_2 := -\frac{m^3 m^2}{2\Lambda^2} + \mu \bar{V} + \mu^2 (V_{21} + V_{22}),$$

where

$$V := \frac{mM}{\sqrt{r'^2 + 2r'a\varrho \cos(g + \nu) + a^2\varrho^2}}$$

and so

$$\begin{aligned} \bar{V} = & \int_0^{2\pi} (1 - e \cos \zeta) \cdot \\ & \cdot \frac{mM}{\sqrt{r'^2 + 2r'a(\cos g(\cos \zeta - e) - \sin g \sqrt{1 - e^2} \sin \zeta) + a^2(1 - e \cos \zeta)^2}} d\zeta. \end{aligned}$$

Then, noticing that $\partial_\Lambda \frac{1}{\omega} = \frac{3\Lambda^2}{m^3 M^2}$, we can express V_{21} as

$$\begin{aligned} V_{21} = & -\frac{1}{4\pi} \left(\frac{3\Lambda^2}{m^3 M^2} \int_0^{2\pi} (1 - e \cos \zeta)(\tilde{V}^2 - \bar{V}) d\zeta + \right. \\ & \left. + \frac{1}{\omega} \int_0^{2\pi} -\frac{G^2}{e\Lambda^3} \cos \zeta (\tilde{V}^2 - \bar{V}) + (1 - e \cos \zeta)(\tilde{V}^2 - \bar{V}) d\zeta \right) \end{aligned}$$

and V_{22} as

$$\begin{aligned} V_{22} = & \frac{1}{4\pi\omega} \left(-\frac{1}{\pi} \int_0^{2\pi} d\zeta \int_0^{\zeta - e \sin \zeta} dp \int_0^{2\pi} dv (1 - e \cos \zeta) \right. \\ & \cdot (1 - e \cos p) \partial_g \tilde{V}(v) \partial_G \tilde{V}(v) \partial_g \tilde{V}(v - p) + \\ & \left. + \int_0^{2\pi} d\zeta \int_0^{2\pi} dp (1 - e \cos \zeta) (1 - e \cos p) \partial_G \tilde{V}(v) \partial_g \tilde{V}(v - p) \right). \end{aligned}$$

Plotting the level sets of H_2 we get phase portraits which are very similar to what we got at the first order, and those are collected in the following subparagraph.

Level Sets of H_2

The following pictures were obtained³ using the Matlab Code reported in A.1.2. They represents the level sets of H_2 in the plane (g, G) . Notice the particular behaviour of the level sets very close to the separatrix: this phenomenon is due to numerical errors, since on the separatrix the denominator of V goes to zero, and it was also present in the first order, but it was hidden by choosing energy values so that the corresponding level sets were not close to the separatrix. Here such choice was not possible.

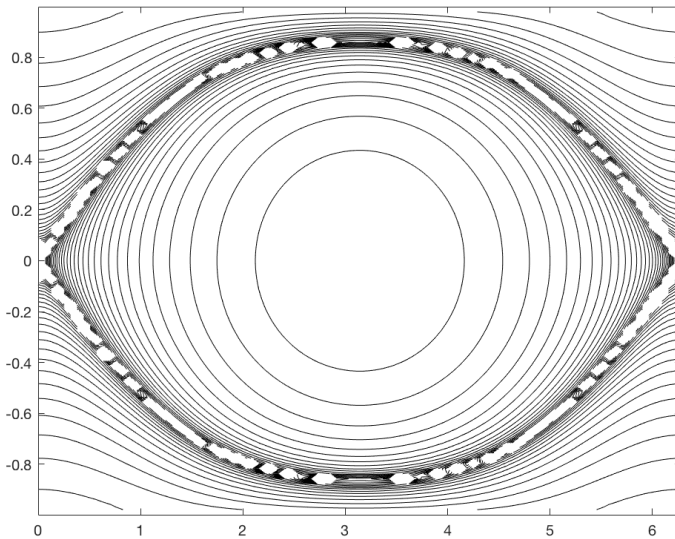


Figure 3.4: Case $\delta \in (0, 1)$, here it is shown the particular case $\delta = \frac{1}{2}$.

³Each picture needed roughly 5 and a half hours to complete on a desktop computer with a Intel Core i7-6700 CPU.

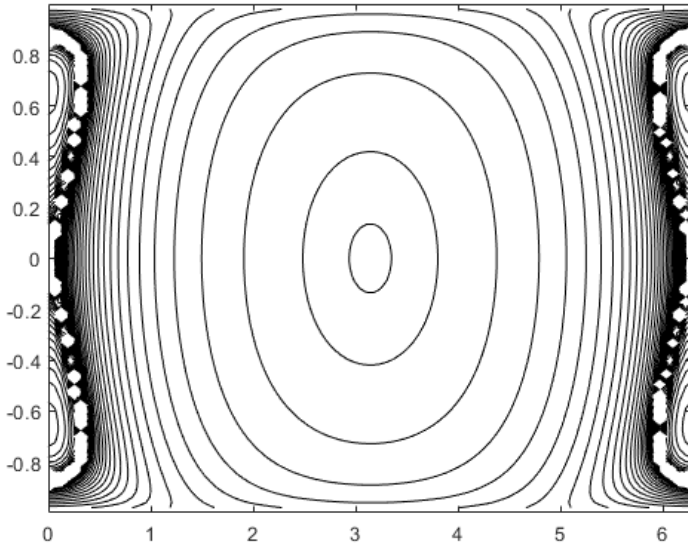


Figure 3.5: Case $\delta \in (1, 2)$, here it is shown the particular case $\delta = \frac{3}{2}$.

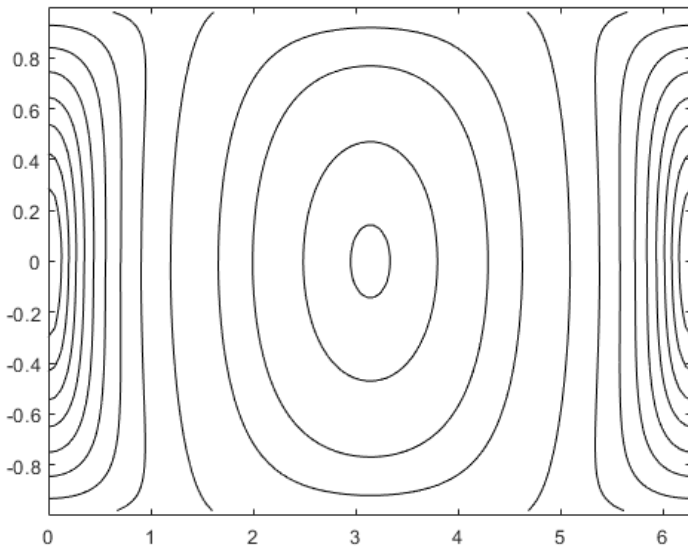


Figure 3.6: Case $\delta > 2$, here it is shown the particular case $\delta = \frac{5}{2}$.

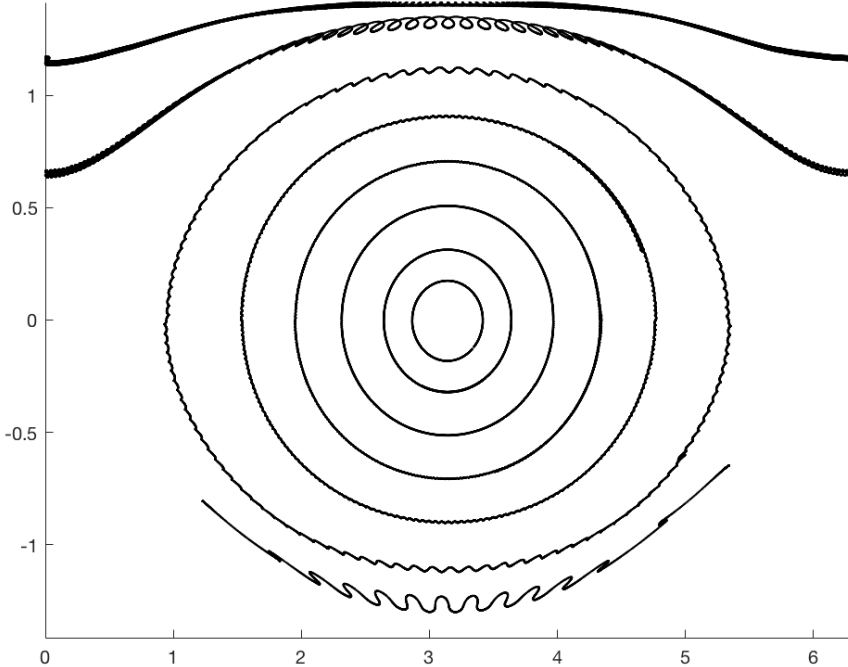


Figure 3.7: Projection of the motion in the (g, G) plane for the *two centre problem*, relative to the values of the parameters $\mu = 10^{-2}$, $\varepsilon = 10^{-7}$, $m_0 = 1$, $C = 10^7$.

3.3 The Full Planar Two-Centre Problem

Setting the parameter σ introduced in chapter 4 to zero allowed us to draw a projection of the motion in the plane (g, G) for the two-centre problem⁴. In this section for every plot the value of the constants is

$$\mu = 10^{-2}, \varepsilon = 10^{-7}, m_0 = 1, C = \varepsilon^{-1}.$$

We report in Figure 3.7 the one relative to $\delta = 0.505$ and in Figure 3.8 the one relative to $\delta = 1.515$. As far as the other variables are concerned, we report the analysis of a couple of single orbits and the corresponding motion of the free body.

⁴The Matlab code used is reported in A.3.

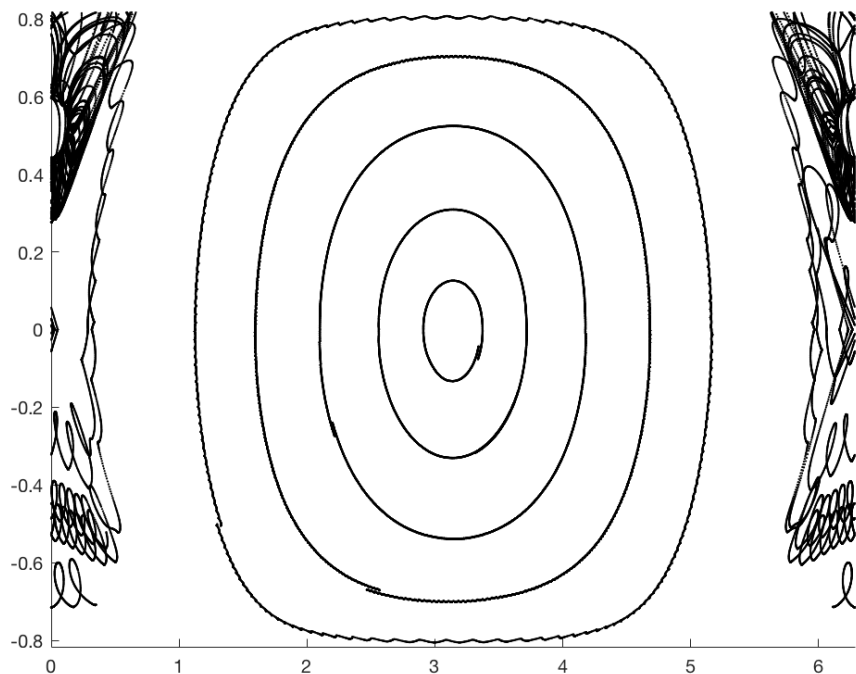


Figure 3.8: Projection of the motion in the (g, G) plane for the *two centre problem* for $\delta = 1.511$, relative to the values of the parameters $\mu = 10^{-2}$, $\varepsilon = 10^{-7}$, $m_0 = 1$, $C = 10^7$.

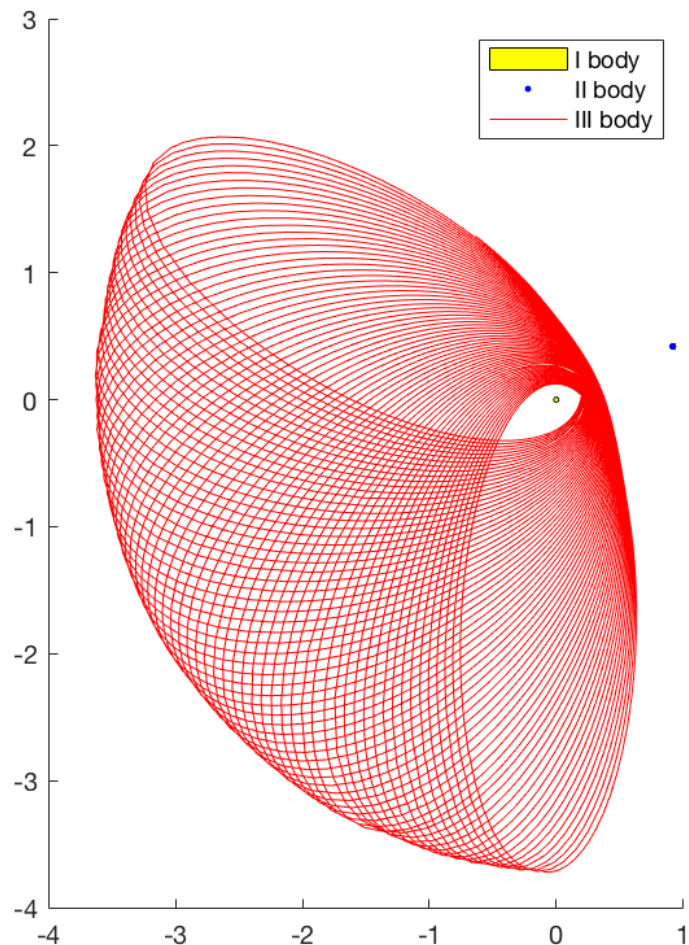


Figure 3.9: The spatial orbit made by the free body in the *two centre problem* for $\delta = 0.505$ and for the initial point $z_0 = (\Lambda_0, \ell_0, G_0, g_0, R'_0, r'_0, \gamma_0) = (\sqrt{2}, 3, 0.8, 1, 0, 1.01, 2)$ on the time interval $(-5 \cdot 10^9, 5 \cdot 10^9)$.

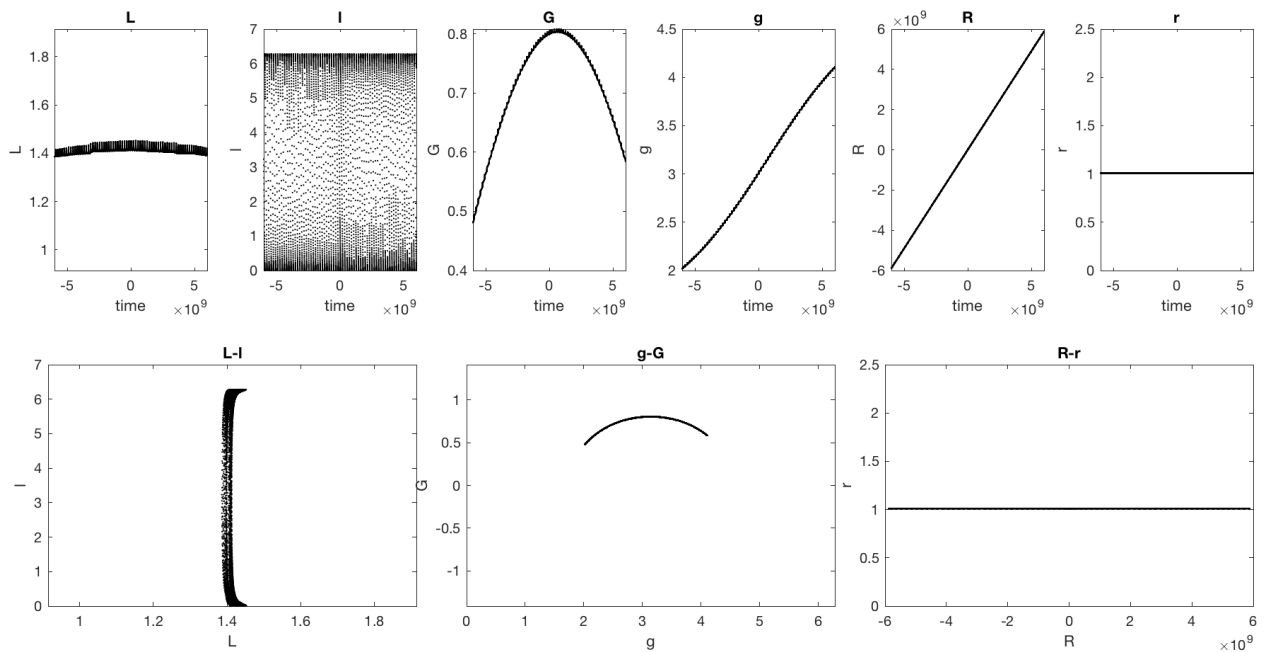


Figure 3.10: The evolution of the variables $(\Lambda, \ell, g, G, r, R)$ for $\delta = 0.505$ along the orbit starting from $z_0 = (\Lambda_0, \ell_0, G_0, g_0, R'_0, r'_0, \gamma_0) = (\sqrt{2}, 3, 0.8, 1, 0, 1.01, 2)$ on the time interval $(-5 \cdot 10^9, 5 \cdot 10^9)$.

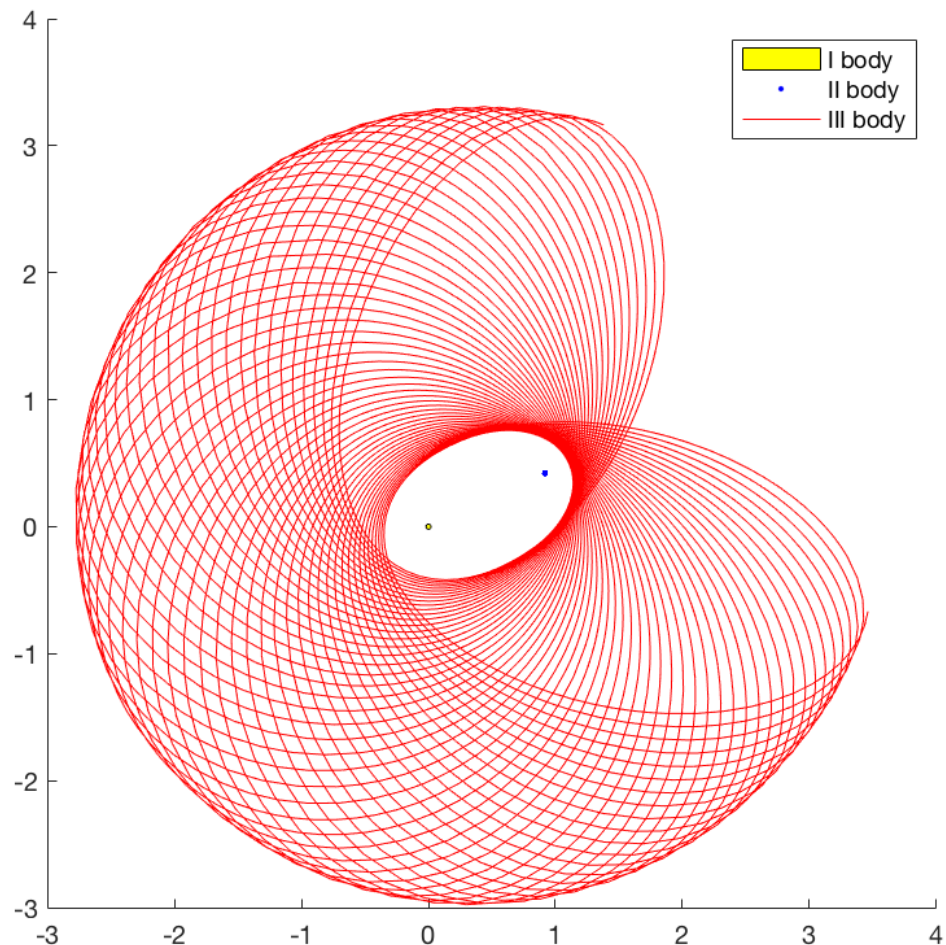


Figure 3.11: The spatial orbit made by the free body in the *two centre problem* for $\delta = 0.505$ and for the initial point $z_0 = (\Lambda_0, \ell_0, G_0, g_0, R'_0, r'_0, \gamma_0) = (\sqrt{2}, 3, 1.3, 1, 0, 1.01, 2)$ on the time interval $(-5 \cdot 10^9, 5 \cdot 10^9)$.

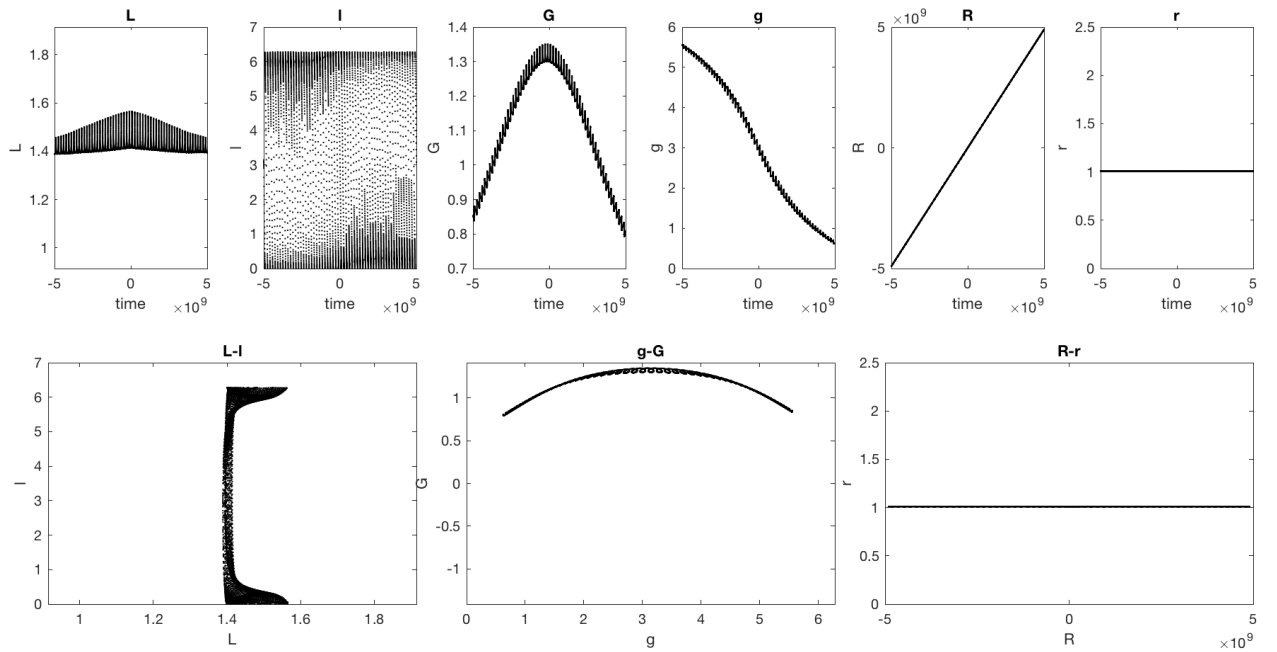


Figure 3.12: The evolution of the variables $(\Lambda, \ell, g, G, r, R)$ for $\delta = 0.505$ along the orbit starting from $z_0 = (\Lambda_0, \ell_0, G_0, g_0, R'_0, r'_0, \gamma_0) = (\sqrt{2}, 3, 1.3, 1, 0, 1.01, 2)$ on the time interval $(-5 \cdot 10^9, 5 \cdot 10^9)$.

Chapter 4

The Full Perturbed System

Consider now the full planar perturbed system with Hamiltonian (2.8). We shall present an analysis of the dynamic of the system based on a numerical integration of the flow. As done in the previous chapter, it will be useful to work with the eccentric anomaly ζ instead of the mean one ℓ , so that we do not need to solve the Kepler equation

$$\zeta - e(\Lambda, G) \sin \zeta = \ell. \quad (4.1)$$

The Hamiltonian (2.8) is a function of the variables $(\Lambda, G, R, \ell, g, r)$. We define $\tilde{H}(\Lambda, G, R', \zeta, g, r')$ as the Hamiltonian (2.8) expressed using the eccentric anomaly:

$$H(\Lambda, G, R', \ell, g, r') = \tilde{H}(\Lambda, G, R', \zeta(\Lambda, G, \ell), g, r'), \quad (4.2)$$

and it holds

$$\tilde{H} = -\frac{m'M'}{r'} + \varepsilon \left(-\frac{m^3 M^2}{2\Lambda^2} + \tilde{V} \right) + \varepsilon^2 f, \quad (4.3)$$

with

$$\tilde{V} := \frac{mM}{\sqrt{r'^2 + 2r'a(\cos g(\cos \zeta - e) - \sin g\sqrt{1 - e^2}\sin \zeta)) + a^2(1 - e\cos \zeta)^2}},$$

and f as in (2.10).

Since the variables $(\Lambda, G, R', \zeta, g, r')$ are not Hamiltonian, we will first need to derive the equations for the Hamiltonian vector field.

Proposition 1. *The equations for the Hamiltonian vector field associated to \tilde{H} are the following:*

$$\left\{ \begin{array}{l} \dot{\Lambda} = \frac{\tilde{H}_\zeta}{1 - \cos \zeta} \\ \dot{G} = \tilde{H}_g \\ \dot{R} = \tilde{H}_r \\ \dot{\zeta} = \frac{1}{1 - e \cos \zeta} \left(\frac{G^2}{e \Lambda^3} \frac{\sin \zeta \tilde{H}_\zeta}{1 - e \cos \zeta} - \frac{G}{e \Lambda^2} \sin \zeta \tilde{H}_g - \left(\tilde{H}_\Lambda + \frac{G^2}{e \Lambda^3} \frac{\sin \zeta \tilde{H}_\zeta}{1 - e \cos \zeta} \right) \right) \\ \dot{g} = -\tilde{H}_G + \frac{G}{e \Lambda^2} \frac{\sin \zeta \tilde{H}_\zeta}{1 - e \cos \zeta} \\ \dot{r} = -\tilde{H}_R. \end{array} \right. \quad (4.4)$$

Proof. From (4.2) and (4.1) it follows that

- $\dot{\Lambda} = H_\ell = \tilde{H}_\zeta \zeta_\ell = \tilde{H}_\zeta \frac{1}{1 - e \cos \zeta}$
- $\dot{G} = H_g = \tilde{H}_g$
- $\dot{R} = H_r = \tilde{H}_r$
- $\dot{\zeta} = \zeta_\Lambda \dot{\Lambda} + \zeta_G \dot{G} + \zeta_\ell \dot{\ell} = \zeta_\Lambda H_\ell + \zeta_G H_g - \zeta_\ell H_\Lambda$ where ζ_Λ , ζ_G and ζ_ℓ can be found from deriving (4.1) and recalling that ζ is a function of (Λ, G, ℓ) .

It turns out that

$$\begin{aligned} \zeta_\Lambda &= \frac{e_\Lambda \sin \zeta}{1 - e \cos \zeta} = \frac{G^2}{e \Lambda^3} \frac{\sin \zeta}{1 - e \cos \zeta}, \\ \zeta_G &= \frac{e_G \sin \zeta}{1 - e \cos \zeta} = -\frac{G}{e \Lambda^2} \frac{\sin \zeta}{1 - e \cos \zeta}, \\ \zeta_\ell &= \frac{1}{1 - e \cos \zeta} \end{aligned}$$

while H_ℓ , H_g have been already computed, and $H_\Lambda = \tilde{H}_\Lambda + \tilde{H}_\zeta \zeta_\Lambda$;

- $\dot{g} = -H_G = -\tilde{H}_G - \tilde{H}_\zeta \zeta_G$, and finally
- $\dot{r} = -H_R = -\tilde{H}_R$.

□

We add to the equations in (4.4) the component relative to the angle γ , which is the variable conjugated to C , so it holds

$$\dot{\gamma} = -H_C.$$

This angle will be useful for plotting the spatial configuration of the three bodies during the motion, since it appears in the formulae (2.13).

In order to better understand the contribution of the perturbation to the dynamic of the system we introduced in our programs a parameter σ in place of ε^2 in the Hamiltonian (4.3), so that we could introduce the perturbation gradually.

We used Mathematica¹ in order to derive the explicit formula of the Hamiltonian vector field. We have then solved numerically the Hamiltonian ODEs using the Matlab Code reported in A.2.3.

In order to have a feedback on our analysis, we always checked the conservation of the Hamiltonian H along a solution. This has been done by computing the norm of the difference between a vector \mathbf{v}_0 with each component being constantly equal to the value of the energy H at the initial point and another vector \mathbf{v} formed by the value of the energy on each point of the calculated orbit.

4.1 Numerical Results

We now present some of the results we obtained varying the parameters. We will call z_0 the initial value:

$$z_0 = (\Lambda_0, \ell_0, G_0, g_0, R'_0, r'_0),$$

and with δ_0 the initial value of δ .

We found that in order to have the conservation of the energy along an orbit it seems to be necessary that $C \sim \frac{1}{\varepsilon}$.

For the moment consider this choice of the parameters:

$$\mu = 10^{-2}, \varepsilon = 10^{-7}, m_0 = 1, C = 10^7.$$

¹The Mathematica Notebook used is reported in A.2.1.

We define r'_0 as the value of r' that corresponds to the circular motions of the second body²:

$$r'_0 := \varepsilon^2 \frac{(C - G)^2}{M'm'^2}.$$

We report in Figure 4.1, Figure 4.2 and Figure 4.3 three phase portraits in the plane in the plane (g, G) for increasing values of σ . The orbits drawn corresponds to the initial points

$$(\Lambda_0, \ell_0, G_0, g_0, R'_0, r'_0) = (\sqrt{2}, 3, G, 2.8, 0, \varepsilon^2 \frac{(C - G)^2}{M'm'^2}),$$

with $G = 0.1, 0.3, 0.5, 0.7, 0.9, 1.1, 1.3, -1.3, -\Lambda + 0.1$. We can see that for $\sigma = \varepsilon^4$ the variation from the phase portrait of the two-centre problem in Figure 3.7 is very minimal. Already with $\sigma = \varepsilon^3$ we see that some of the orbits below the separatrix start to open up into lines, and finally with $\sigma = \varepsilon^2$ we see that the true perturbation alters radically the projection of the motion in the plane (g, G) . Lowering the value of ε has the effect of making the lines in the (g, G) plane more defined, as can be seen in Figure 4.4. The same behaviour is also true for higher values of δ_0 .

In the next pages we report the evolution of all variables and the spatial configuration of the three bodies in the for a couple of particular

4.1.1 Collisions

Collision of the Second Body with the First One

We found that starting from the initial value $z_0 = (\sqrt{2}, 1, 0.5, 3, 0, 0.3r'_0, 2)$, and integrating on the time span $(-3 \cdot 10^8, 3 \cdot 10^8)$ yields to a collision of the second body with the first one, as seen in Figure 4.11. The parameters had been chosen as follows: $\mu = 10^{-3}$, $\varepsilon = 10^{-7}$, $\sigma = \varepsilon^2$, $C = 1.2\varepsilon^{-1}$. As expected, the conservation of the energy does not hold in this case. The evolution of all variables is reported in 4.12 For this particular case we also report the evolution of δ , of the first integral J and the evolution of the eccentricity of the third body on every point of the orbit, respectively in Figure 4.13, in Figure 4.14 and in Figure 4.15. This behaviour holds for every value of G .

²Such value of r'_0 corresponds to the value of r' for which the potential

$$-\varepsilon \frac{mM}{r'} + \varepsilon^2 \frac{(C - G)^2}{2r'm'}$$

reaches its minimum point.

Collision of the Third Body with the First One

Starting from an initial point close to the separatrix³ yields to a collision of the third body with the first one. We analysed a special case, namely the orbit starting from the initial point

$$(\sqrt{2}, 1, 0.01, 0.01, 0, \varepsilon^2 \frac{(C - G)^2}{m'^2 M}, 2),$$

leaving the parameters with the same values that had been fixed in the previous subsection. We thus report all the graphics that we reported for the collision of the second body with the comparison in Figure 4.16, Figure 4.17, Figure 4.18, in Figure 4.19 and in Figure 4.20.

³Which we recall being the level set through the point $(g, G) = (0, 0)$.

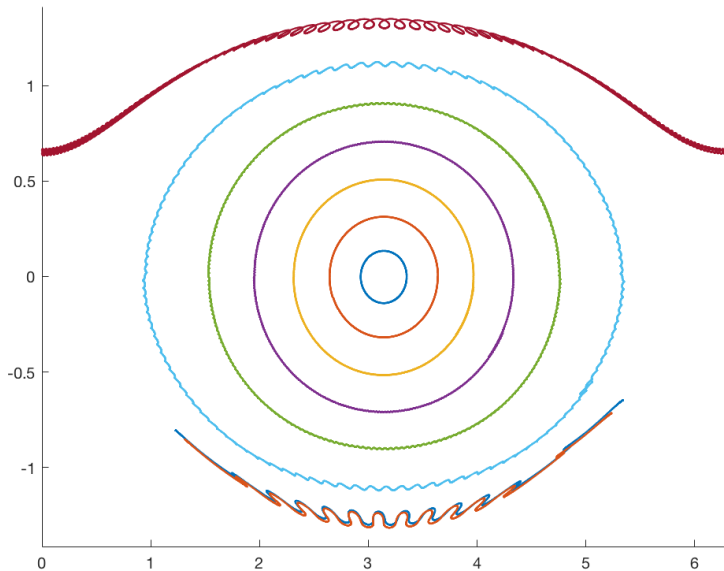


Figure 4.1: Projection of the motion in the plane (g, G) for $\sigma = \varepsilon^4$.

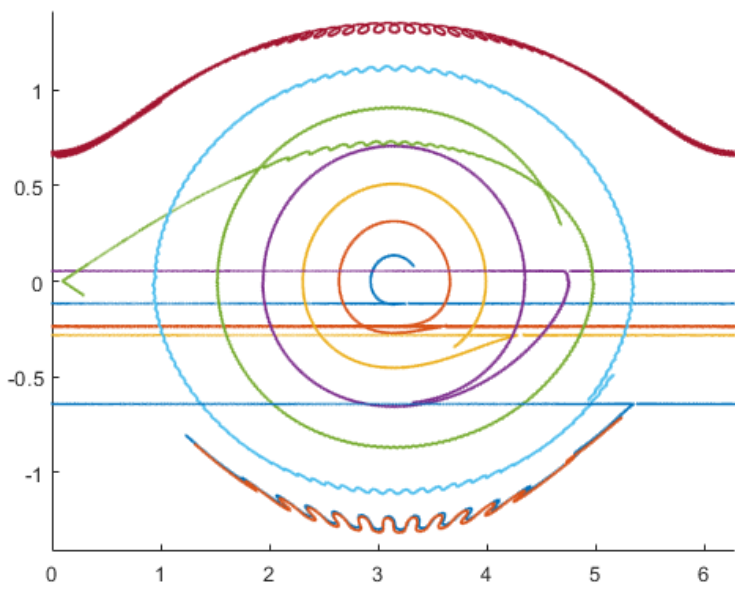


Figure 4.2: Projection of the motion in the plane (g, G) for $\sigma = \varepsilon^3$.

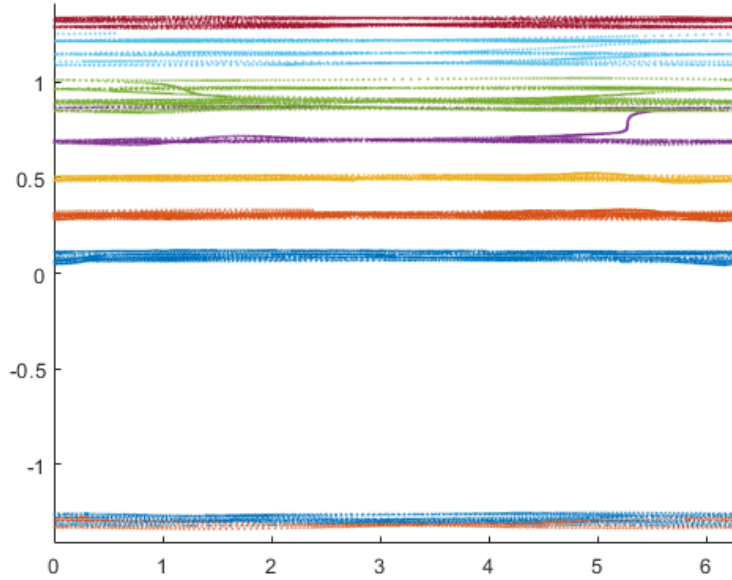


Figure 4.3: Projection of the motion in the plane (g, G) for $\sigma = \varepsilon^2$.

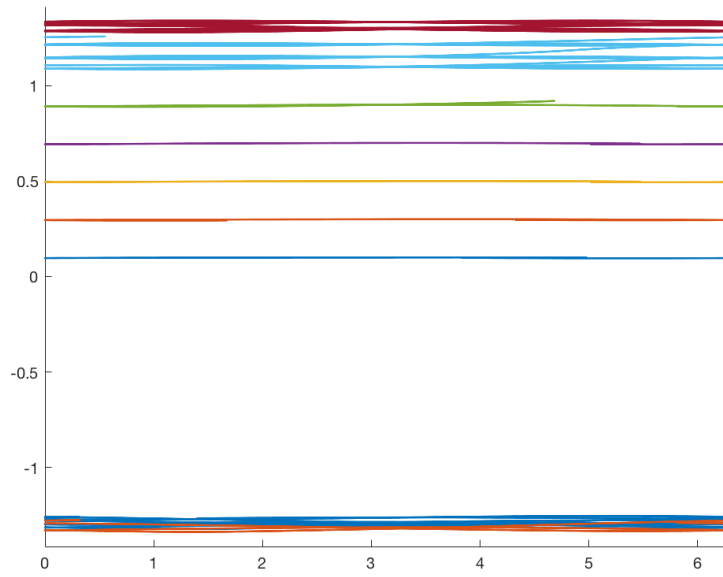


Figure 4.4: Projection of the motion in the plane (g, G) for $\sigma = \varepsilon^2$ and $\varepsilon = 10^{-11}$.

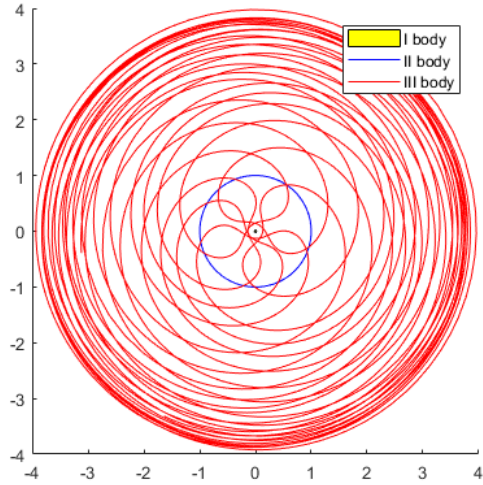


Figure 4.5: Spatial configurations of the three bodies for $\delta_0 = 0.505$, $\sigma = \varepsilon^2$ with $\mu = 10^{-3}$, $\varepsilon = 10^{-7}$, $C = \varepsilon^{-1}$ on the time interval $(-5 \cdot 10^8, 5 \cdot 10^8)$ relative to the initial point $(\sqrt{2}, 3, 0.5, 3, 0, \varepsilon^2 \frac{(C-G)^2}{m'^2 M}, 2)$.

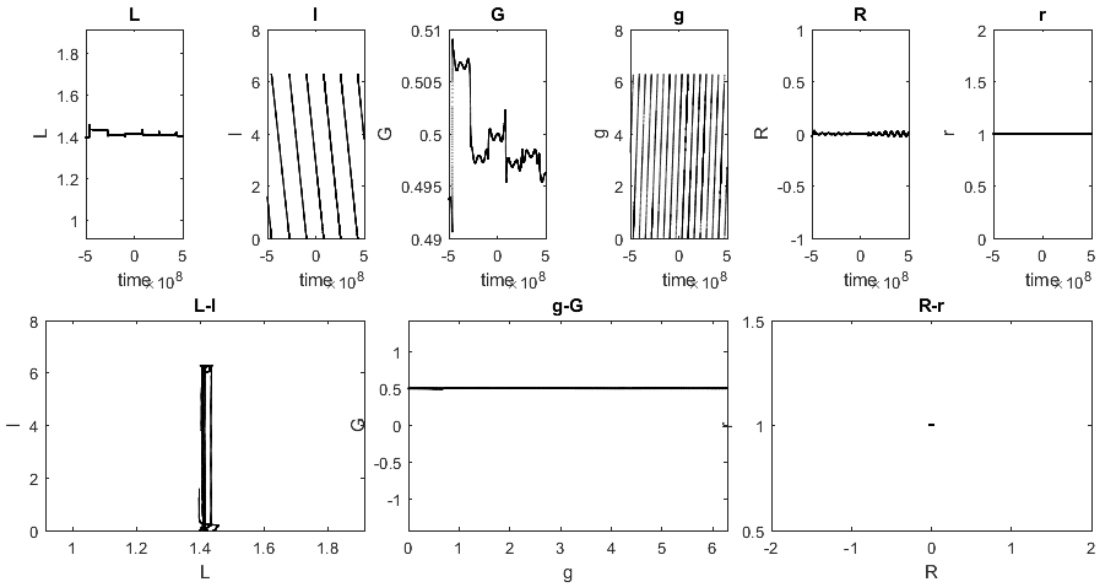


Figure 4.6: The evolution of all variables corresponding to the orbit for $\delta_0 = 0.505$, $\sigma = \varepsilon^2$ with $\mu = 10^{-3}$, $\varepsilon = 10^{-7}$, $C = \varepsilon^{-1}$ on the time interval $(-5 \cdot 10^8, 5 \cdot 10^8)$ relative to the initial point $(\sqrt{2}, 3, 0.5, 3, 0, r'_0, 2)$.

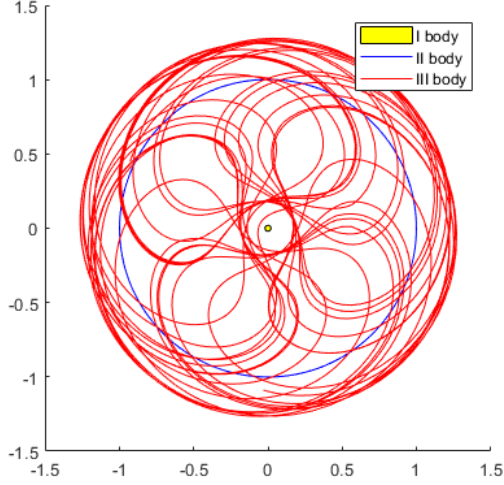


Figure 4.7: Spatial configurations of the three bodies for $\delta_0 = 1.515, \sigma = \varepsilon^2$ with $\mu = 10^{-3}, \varepsilon = 10^{-7}, C = \varepsilon^{-1}$ on the time interval $(-5 \cdot 10^8, 5 \cdot 10^8)$ relative to the initial point $(\sqrt{2}, 3, 0.5, 3, 0, \varepsilon^2 \frac{(C-G)^2}{m'^2 M}, 2)$.

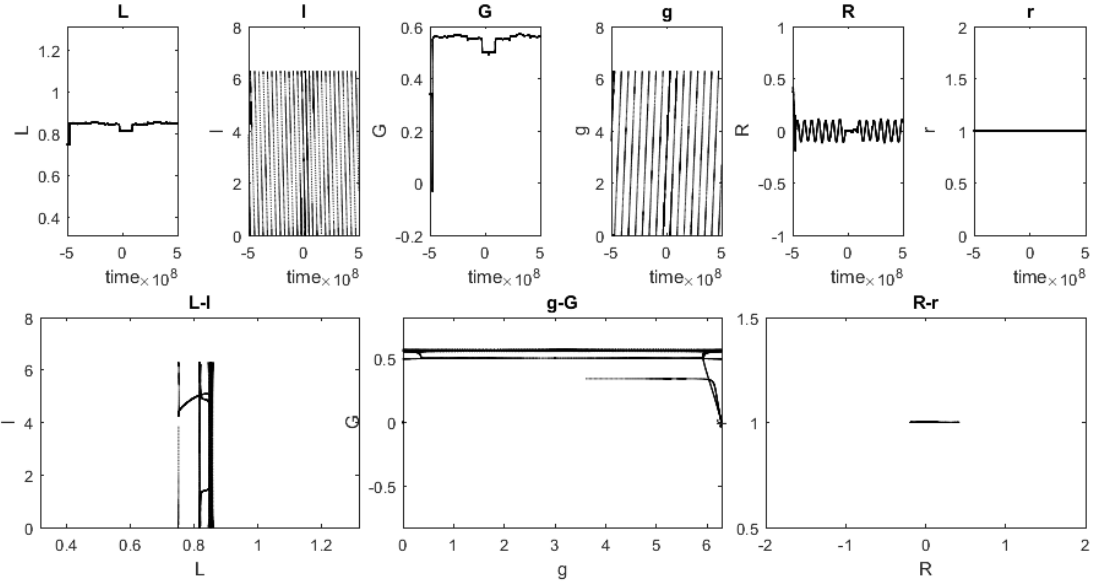


Figure 4.8: The evolution of all variables corresponding to the orbit for $\delta_0 = 1.515, \sigma = \varepsilon^2$ with $\mu = 10^{-3}, \varepsilon = 10^{-7}, C = \varepsilon^{-1}$ on the time interval $(-5 \cdot 10^8, 5 \cdot 10^8)$ relative to the initial point $(\sqrt{2}, 3, 0.5, 3, 0, \varepsilon^2 \frac{(C-G)^2}{m'^2 M}, 2)$.

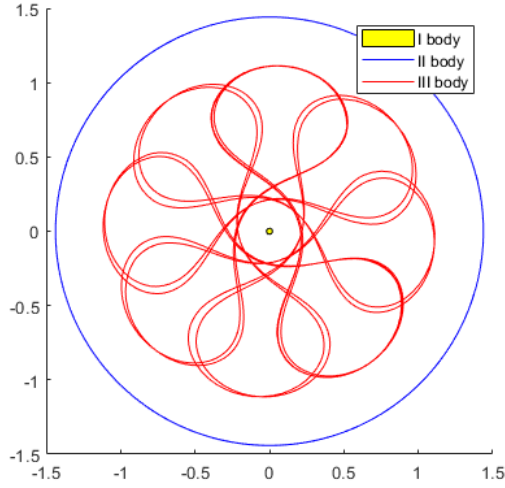


Figure 4.9: Spatial configurations of the three bodies for $\delta_0 = 1.515$, $\sigma = \varepsilon^2$ and $C = 1.2\varepsilon^{-1}$. with $\mu = 10^{-3}$, $\varepsilon = 10^{-7}$, $C = \varepsilon^{-1}$ on the time interval $(-3 \cdot 10^8, 3 \cdot 10^8)$ relative to the initial point $(\sqrt{2}, 3, 0.3, 3, 0.5, 0.7r'_0, 2)$.

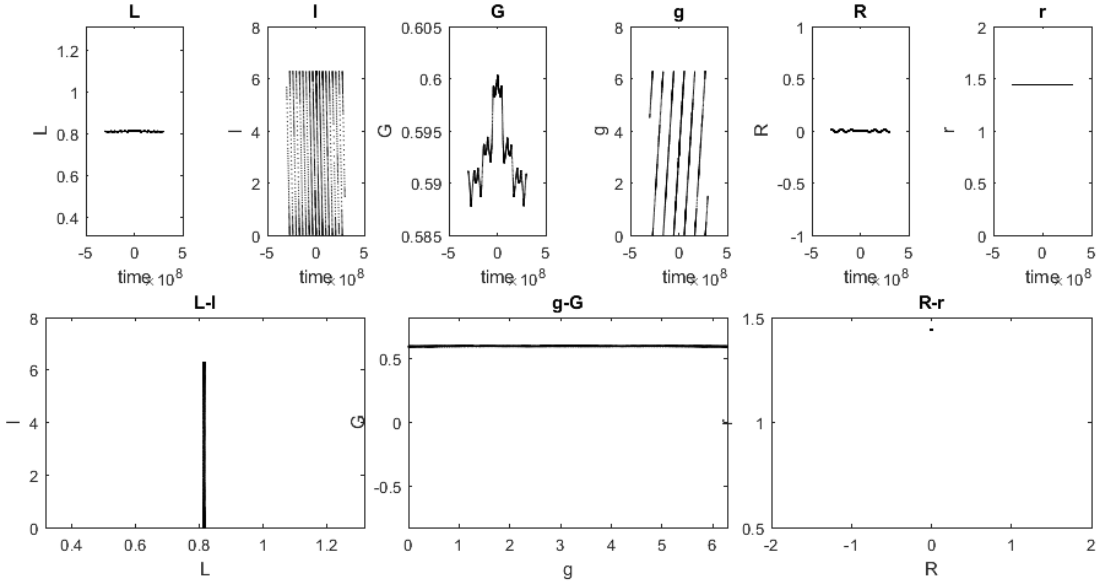
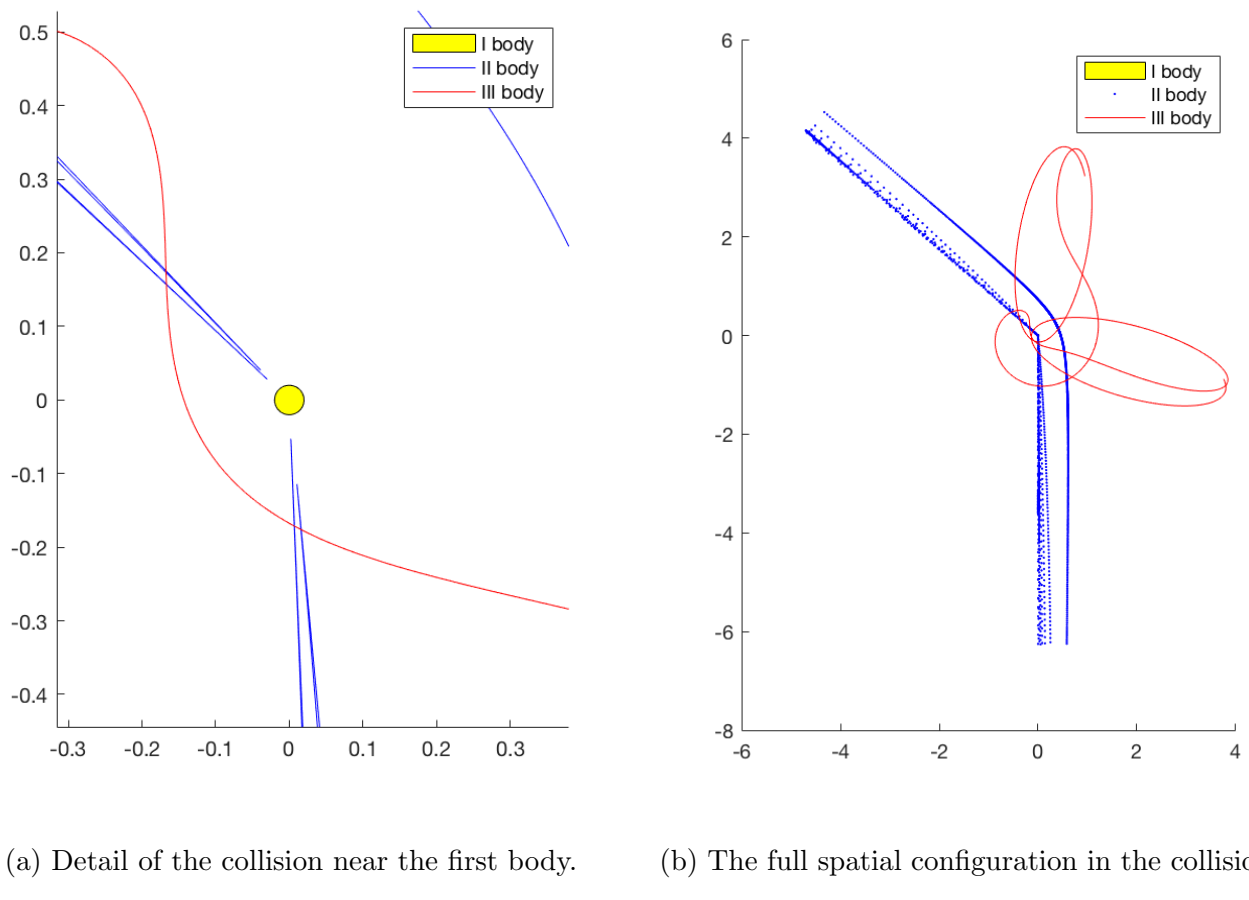


Figure 4.10: The evolution of all variables corresponding to the orbit for $\delta_0 = 1.515$, $\sigma = \varepsilon^2$ and $C = 1.2\varepsilon^{-1}$. with $\mu = 10^{-3}$, $\varepsilon = 10^{-7}$, $C = \varepsilon^{-1}$ on the time interval $(-3 \cdot 10^8, 3 \cdot 10^8)$ relative to the initial point $(\sqrt{2}, 3, 0.3, 3, 0.5, 0.7r'_0, 2)$.



(a) Detail of the collision near the first body.

(b) The full spatial configuration in the collision.

Figure 4.11: Spatial configuration of the three bodies during a collision of the second body with the first one.

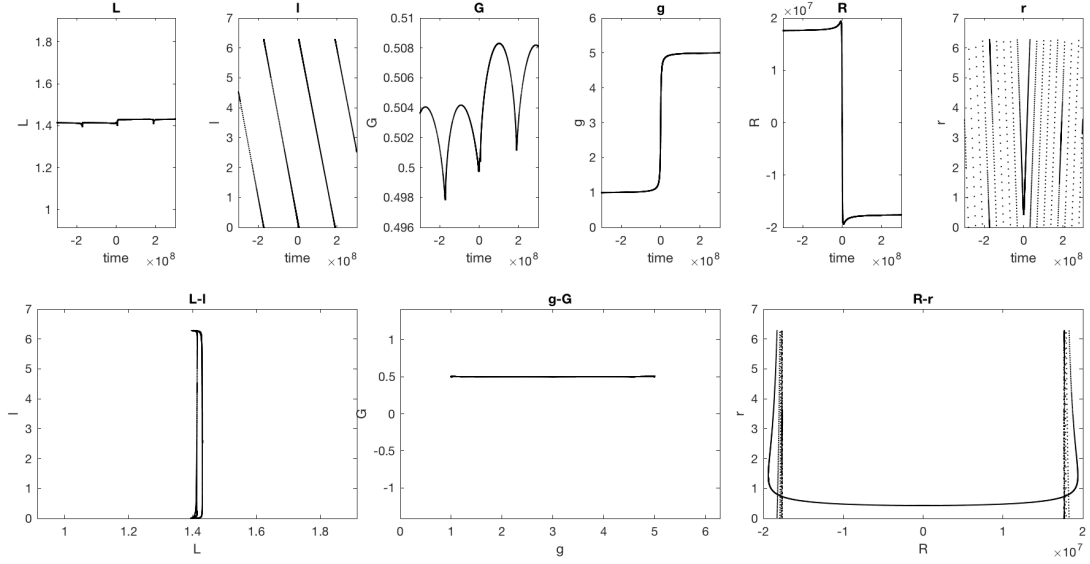


Figure 4.12: The evolution of all variables corresponding to a collision of the second body with the first one. The value of the parameters are and $\mu = 10^{-3}$, $\varepsilon = 10^{-7}$, $\sigma = \varepsilon^2$, $C = 1.2\varepsilon^{-1}$. The time interval $(-3 \cdot 10^8, 3 \cdot 10^8)$. The initial point is $(\sqrt{2}, 1, 0.5, 3, 0, 0.7r'_0, 2)$.

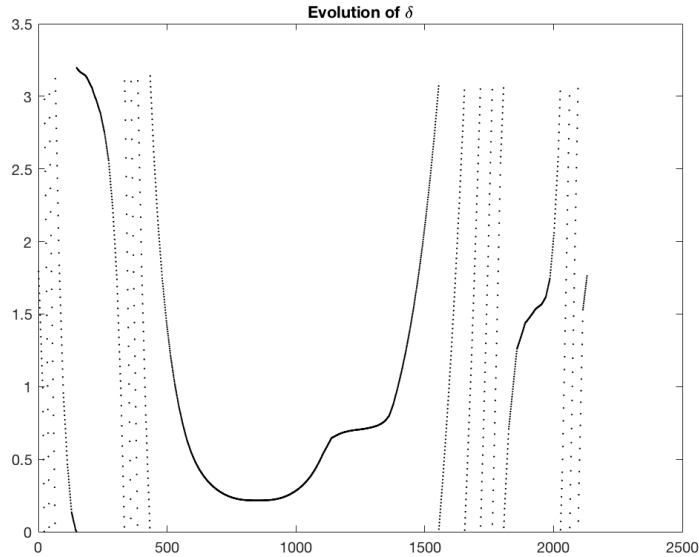


Figure 4.13: Evolution of the value of the parameter δ during the motion.

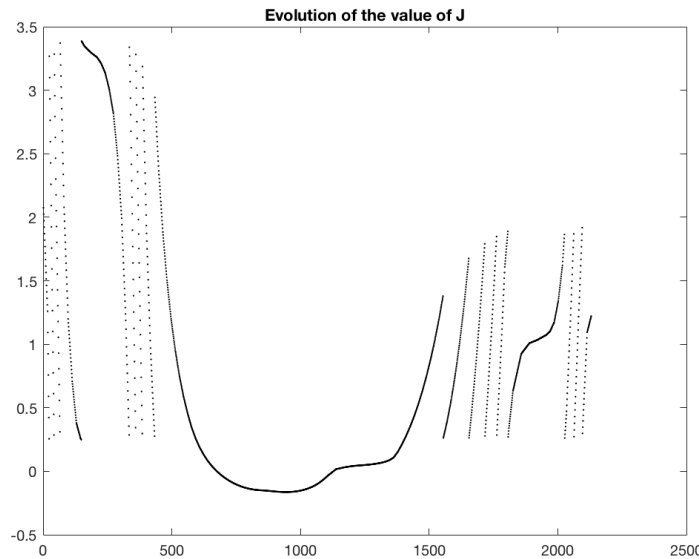


Figure 4.14: Evolution of the value of the first integral J during the motion.

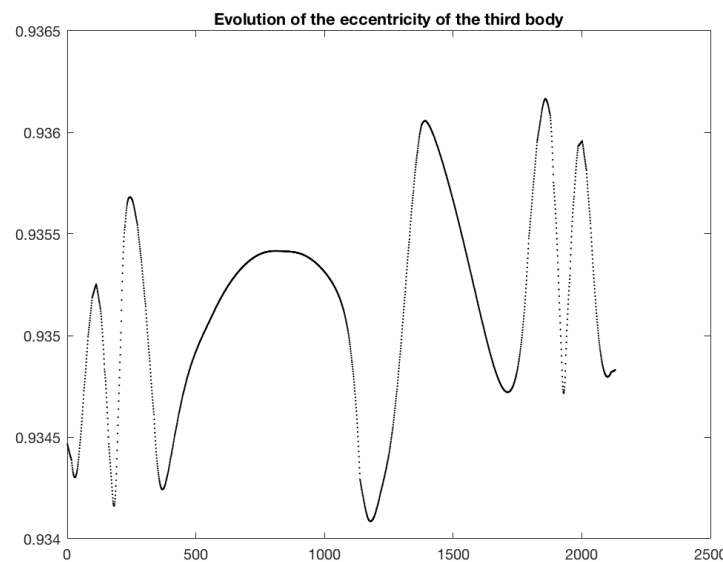
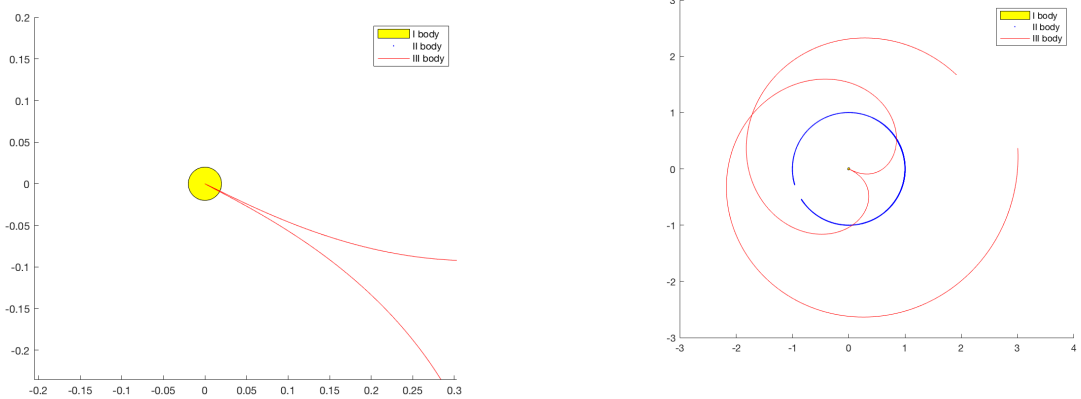


Figure 4.15: Evolution of the eccentricity of the third body during the motion.



(a) Detail of the collision near the first body.

(b) The full spatial configuration in the collision.

Figure 4.16: Spatial configuration of the three bodies during a collision of the second body with the first one.

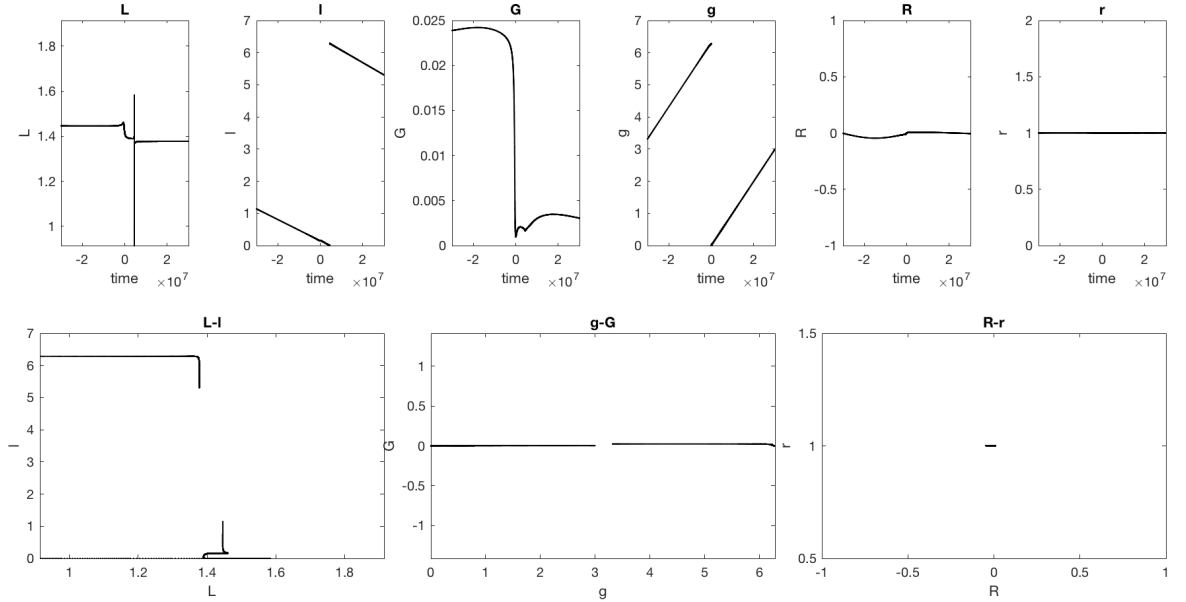


Figure 4.17: The evolution of all variables corresponding to a collision of the third body with the first one. The value of the parameters are and $\mu = 10^{-3}, \varepsilon = 10^{-7}, \sigma = \varepsilon^2, C = \varepsilon^{-1}$. The time interval $(-3 \cdot 10^7, 3 \cdot 10^7)$. The initial point is $(\sqrt{2}, 1, 0.01, 0.01, 0, \varepsilon^2 \frac{(C-G)^2}{m'^2 M}, 2)$.

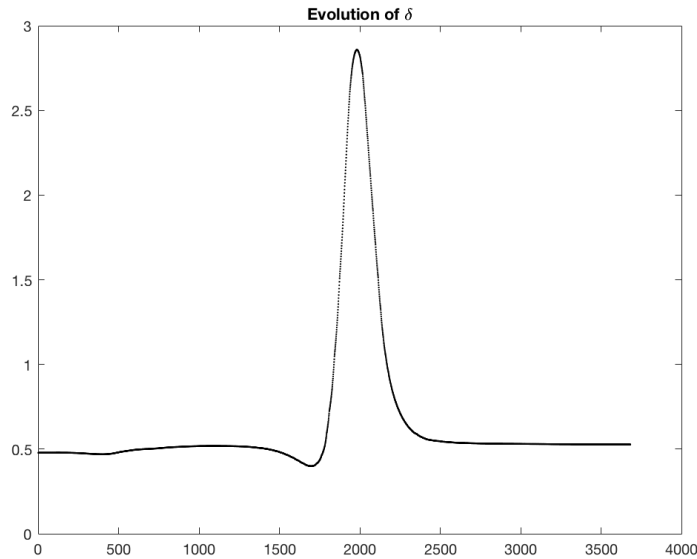


Figure 4.18: Evolution of the value of the parameter δ during the motion.

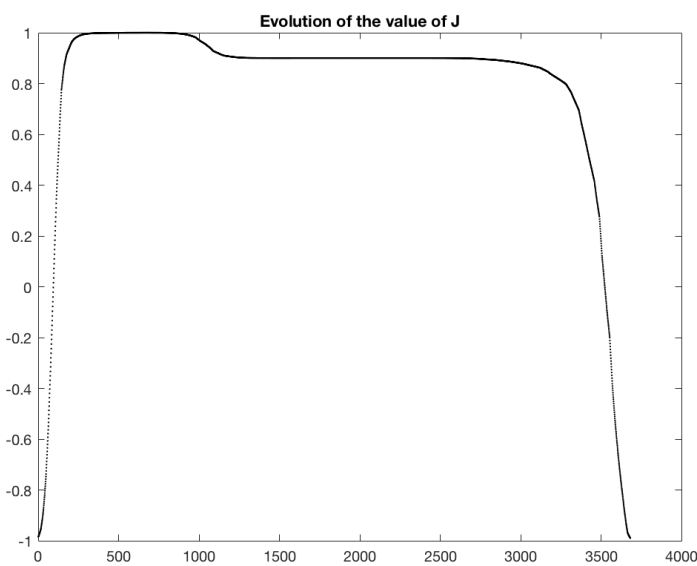


Figure 4.19: Evolution of the value of the first integral J during the motion.

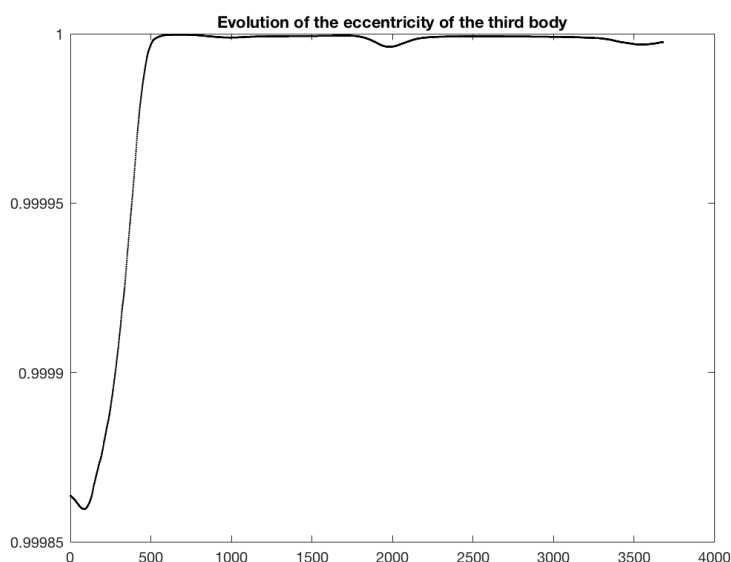


Figure 4.20: Evolution of the eccentricity of the third body during the motion.

Appendices

Appendix A

Code

We will collect here the code used to obtain the graphics in the thesis. The code was written mainly in Matlab¹, but very often it was useful to first make some symbolic manipulations in Mathematica² in order to derive the formulae, and then to export them in Matlab Code using the Mathematica ToMaltab.m package³. When relevant, we will also provide the Mathematica Code.

A.1 Unperturbed System

A.1.1 First Perturbation Step

```
1 function [Uc]=phase_portrait_step1(delta)
2 f=@(u,delta,g,G)
3 (-1/2).*delta.*pi.^(-1).* (1+(-1).* (1+(-1).*G.^2).^(1/2).*cos(u)).*(...
4 delta.^2+(1+(-1).* (1+(-1).*G.^2).^(1/2).*cos(u)).^2+2.*delta.* (cos(g).*...
5 (-1).* (1+(-1).*G.^2).^(1/2)+cos(u))+(-1).*G.*sin(g).*sin(u))).^(-1/2);
6 %The first order averaged energy.
7 U=@(g,G) integral(@(u) f(u,delta,g,G),0,2.*pi);
8 %The level sets.
9 Uc=fcontour(U,[0,2*pi,-1,1])
10 Uc.LineColor='Black';
```

¹The MathWorks, Inc., *Matlab*, Version R2018a, Natick, MA, USA (2018)

²Wolfram Research, Inc., *Mathematica*, Version 11.3, Champaign, IL (2018).

³This package is available at <http://library.wolfram.com/infocenter/MathSource/577/>.

```

11 Uc.MeshDensity=100;
12 end

```

A.1.2 Second Perturbation Step

```

1 function phase_portrait_step2(delta)
2 % We fix the parameters.
3 a=1; r=delta; m=(1+10E-6).^-1; M=1+10E-6; L=m*sqrt(M*a); ...
4 mi=10^-4;
5 h=-(m.^3*M.^2)/(2.*L.^2);
6 omega=(m.^3*M.^2)./L.^3;
7 %the inverse of the derivative of omega with respect to L.
8 invomegaL=3.*L.^2.*m.^(-3).*M.^(-2);
9
10 % The eccentricity
11 e=@(L,G)sqrt(1-(G.^2)./(L.^2));
12
13 % The "perturbation"
14 f =@(g,G,u) (-m.*M)./(sqrt(r.^2+2.*a.*r.*cos(g).*...
15 (cos(u)-e(L,G))-sqrt(1-e(L,G).^2).*sin(g).*sin(u))+...
16 a.^2.*((1-e(L,G).*cos(u)).^2));
17
18 % The derivatives of f needed in the second perturbation step
19 fquadroL=@(g,G,u) (-2).*a.*L.^(-3).*m.^2.*M.^2.*...
20 ((-1).*G.^2.*((1+(-1).*G.^2.*L.^(-2)).^(-1/2).*...
21 r.*cos(g)+a.*G.^2.*cos(u).*(((-1).*(1+(-1).*G.^2.*L.^(-2)).^(-1/2)+cos(u))...
22 +(G.^2.*L.^(-2)).^(1/2).*L.^2.*r.*sin(g).*sin(u)).*(r.^2+(a+(-1)...
23 .*a.*((1+(-1).*G.^2.*L.^(-2)).^(1/2).*cos(u)).^2+2.*a.*r.*cos(g).*(((-1)...
24 .*((1+(-1).*G.^2.*L.^(-2)).^(1/2)+cos(u))+(-1).*((G.^2.*L.^(-2)).^(1/2).*...
25 sin(g).*sin(u))).^(-2));
26 fL=@(g,G,u) a.*L.^(-3).*m.*M.*((-1).*G.^2.*...
27 ((1+(-1).*G.^2.*L.^(-2)).^(-1/2).*r.*cos(g)+a.*G.^2.*cos(u).*(((-1).*...
28 (1+(-1).*G.^2.*L.^(-2)).^(-1/2)+cos(u))...
29 +(G.^2.*L.^(-2)).^(1/2).*L.^2.*r.*sin(g).*sin(u)).*...
30 (r.^2+(a+(-1).*a.*((1+(-1).*G.^2.*L.^(-2)).^(1/2).*cos(u))...
31 .^2+2.*a.*r.*cos(g).*(((-1).*((1+(-1)...
32 .*G.^2.*L.^(-2)).^(1/2)...
33 +cos(u))+(-1).*((G.^2.*L.^(-2)).^(1/2).*sin(g).*sin(u))).^(-3/2);
```

```

32 fg=@(g,G,u) a.*m.*M.*r.*(((1+(-1).*G.^2.*L.^(-2)).^(1/2)...
33      +(-1).*cos(u)).*sin(g)+(-1).* (G.^2.*L.^(-2)).^(1/2).*...
34      cos(g).*sin(u)).*(r.^2+(a+(-1).*a.* (1+(-1).*...
35      G.^2.*L.^(-2)).^(1/2).*cos(u)).^2+2.*a.*r.* (cos(g).* ((-1).* (1+(-1).*...
36      G.^2.*L.^(-2)).^(1/2)+cos(u))+(-1).*...
37      (G.^2.*L.^(-2)).^(1/2).*sin(g).*sin(u))).^(-3/2);
38 fG=@(g,G,u) (1/2).*m.*M.* (2.*a.*G.* (1+(-1).*G.^2.*...
39      L.^(-2)).^(1/2).*L.^(-2).*r.*cos(g)+2.*a.^2.*G.*L.^(-2).*...
40      ((1+(-1).*G.^2.*L.^(-2)).^(1/2)+(-1).*cos(u)).*cos(u)+(-2).*...
41      a.*G.^(-1).* (G.^2.*L.^(-2)).^(1/2).*r.*sin(g).*sin(u)).*...
42      (r.^2+(a+(-1).*a.* (1+(-1).*G.^2.*L.^(-2)).^(1/2).*cos(u)).^2...
43      +2.*a.*r.* (cos(g).* ((-1).* (1+(-1).*G.^2.*L.^(-2)).^(1/2)+cos(u))...
44      +(-1).* (G.^2.*L.^(-2)).^(1/2).*sin(g).*sin(u))).^(-3/2);
45
46 % The first part of the second order term
47 term21=@(g,G) -0.5.* (invomegaL.* ((1/(2.*pi)).*integral(@(u)...
48      (1-e(L,G).*cos(u)).*(f(g,G,u).^2-f(g,G,u)),0,2.*pi))...
49      +omega.^(-1).* (2.*pi).^(-1).*integral(@(u) ...
50      -(G.^2).*cos(u)...
51      /(L.^3.*e(L,G)).*(1-e(L,G).*cos(u)).*(f(g,G,u).^2 ...
52      -f(g,G,u))+...
53      (1-e(L,G).*cos(u)).*(fquadroL(g,G,u)-fL(g,G,u)),0,2.*pi));
54
55 % The second part of the second order term
56 int1=@(g,G,u,p,v) ...
57      (1-e(L,G).*cos(u)).*(1-e(L,G).*cos(p)).*fG(g,G,v).*fg(g,G,v-p);
58 int2=@(g,G,u,p) ...
59      (1-e(L,G).*cos(u)).*(1-e(L,G).*cos(p)).*fG(g,G,p).*fg(g,G,p-u);
60 term22=@(g,G) ...
61      (4.*pi.*omega).^(-1)*(pi.^(-1).*integral3(@(u,p,v) ...
62      int1(g,G,u,p,v),...
63      0,2.*pi,0,@(u) u-e(L,G).*sin(u),0,2*pi)+integral2(@(u,p) ...
64      int2(g,G,u,p),0,2*pi,0,2*pi));
65
66 % The second order hamiltonian
67 H2=@(g,G) h+mi.*integral(@(u)f(g,G,u),0,2*pi)+...
68      (mi.^2)*(term21(g,G)+term22(g,G));
69
70
71
72
73

```

```

64 % Grid on the (g,G) plane
65 gv=linspace(0,2*pi,100);
66 Gv=linspace(-L,L,100);
67 [X,Y]=meshgrid(gv,Gv);
68
69 % Values of H2 over the grid
70 Z=zeros(100);
71 parfor i=1:100
72     for j=1:100
73         Z(i,j)=H2(gv(i),Gv(j));
74     end
75 end
76
77 % Plot of the energy levels
78 figure
79 [C,h]=contour(X,Y,Z.',100);
80 h.LineColor='Black';
81
82 end

```

A.2 The Perturbed System

A.2.1 Derivation of the Hamiltonian Vector Field

In order to derive the formulae for the Hamiltonian vector field in (4.4) we first wrote the following Mathematica Notebook to get a good starting point for the code.

Derivation of Matlab Formulae

We load the ToMatlab package

```
In[1]:= SetDirectory[NotebookDirectory[]];
```

```
In[2]:= << ToMatlab.m
```

The eccentricity is defined as

$$In[3]:= e[\Lambda_-, G_-] := \sqrt{1 - \frac{G^2}{\Lambda^2}}$$

The Hamiltonian of the planar hierarchical three body problem, expressed using the eccentric anomaly ζ and substituting σ in place of ε^2 is the following:

$$\begin{aligned} In[4]:= H3Bs[\{\Lambda_-, \xi_-, G_-, g_-, R_-, r_-\}] := \\ -\frac{m p M p}{r} + \varepsilon \left(\frac{-m^3 M^2}{2 \Lambda^2} + \mu \left((-m M) / \sqrt{r^2 + 2 r \frac{\Lambda^2}{M m^2} (\cos[g] (\cos[\xi] - e[\Lambda, G]) - \right. \right. \\ \left. \left. \sqrt{1 - e[\Lambda, G]^2} \sin[g] \sin[\xi]) + \left(\frac{\Lambda^2}{M m^2} \right)^2 (1 - e[\Lambda, G] \cos[\xi])^2 \right) \right) + \\ \text{sigma} \left(\frac{R^2}{2 m p} + \frac{(n C t - G)^2}{2 r^2 m p} + \frac{\mu}{m \theta} \left(- \left(m^2 M \left(\sin[g] \left(r R \sqrt{\frac{G^2}{\Lambda^2}} \cos[\xi] - \right. \right. \right. \right. \right. \\ \left. \left. \left. \left. \left. \left. (G + n C t) \sin[\xi] \right) + \cos[g] \left((G + n C t) \sqrt{\frac{G^2}{\Lambda^2}} \cos[\xi] + \right. \right. \right. \right. \right. \\ \left. \left. \left. \left. \left. \left. r R \sin[\xi] \right) \right) \right) \right) / \left(-r \Lambda + r \sqrt{1 - \frac{G^2}{\Lambda^2}} \Lambda \cos[\xi] \right) \right); \end{aligned}$$

```
In[5]:= H3Bs[\{\Lambda, \xi, G, g, R, r\}] /.
```

```
{\Lambda \rightarrow a1, \xi \rightarrow a2, G \rightarrow a3, g \rightarrow a4, R \rightarrow a5, r \rightarrow a6, \varepsilon \rightarrow eps, \mu \rightarrow mi};
```

```
In[6]:= WriteMatlab[%,"H3Bs.m"]
```

Derivation of the Hamiltonian vector field:

$$\begin{aligned}
 \text{In[1]:=} & \left\{ \frac{1}{1 - e[\Delta, G] \cos[\xi]} * D[H3Bs[\{\Delta, \xi, G, g, R, r\}], \xi], \right. \\
 & \frac{1}{1 - e[\Delta, G] \cos[\xi]} \left(\frac{\frac{G^2 \sin[\xi]}{\sqrt{1 - \frac{G^2}{\Delta^2}} \Delta^3} * D[H3Bs[\{\Delta, \xi, G, g, R, r\}], \xi] \frac{1}{1 - e[\Delta, G] \cos[\xi]} - \right. \\
 & \frac{\frac{G \sin[\xi]}{\sqrt{1 - \frac{G^2}{\Delta^2}} \Delta^2} D[H3Bs[\{\Delta, \xi, G, g, R, r\}], g] - \\
 & \left. \left(D[H3Bs[\{\Delta, \xi, G, g, R, r\}], \Delta] + D[H3Bs[\{\Delta, \xi, G, g, R, r\}], \xi] \right. \right. \\
 & \left. \left. \frac{G^2 \sin[\xi]}{\sqrt{1 - \frac{G^2}{\Delta^2}} \Delta^3} \frac{1}{1 - e[\Delta, G] \cos[\xi]} \right) \right), \\
 & D[H3Bs[\{\Delta, \xi, G, g, R, r\}], g], -D[H3Bs[\{\Delta, \xi, G, g, R, r\}], G] + \\
 & D[H3Bs[\{\Delta, \xi, G, g, R, r\}], \xi] \frac{\frac{G \sin[\xi]}{\sqrt{1 - \frac{G^2}{\Delta^2}} \Delta^2} \frac{1}{1 - e[\Delta, G] \cos[\xi]}, \\
 & D[H3Bs[\{\Delta, \xi, G, g, R, r\}], r], -D[H3Bs[\{\Delta, \xi, G, g, R, r\}], R], \\
 & \left. -D[H3Bs[\{\Delta, \xi, G, g, R, r\}], nCt] \right\} // Simplify;
 \end{aligned}$$

```

In[1]:= % /. {Δ → a1, ξ → a2, G → a3, g → a4, R → a5, r → a6, ε → eps, μ → mi};

In[1]:= WriteMatlab[%, "vector_field_sigma.m"]

```

Then, we wrote the following Matlab function to declare the constants. Notice that the particular values for mi, eps, sigma and nCt had been changed according to our various attempts.

```

1 function [mi,eps,m0,mp,m,Mp,M,nCt]=constants_sigma()
2     mi = 1E-4; eps = 1E-7;
3     m0 = 1;
4     mp = m0/(1+mi); % corresponding to m'
5     m = m0/(1 + mi*eps);
6     Mp=m0*(1+mi); % corresponding to M'
7     M = m0*(1+eps*mi);
8     sigma=eps^2;
9     nCt=1e7; % corresponding to the C variable
10 end

```

Finally, the Matlab Code obtained polishing the output of Mathematica is the following.

```

1 function y=H3Bs(z0)
2
3 % It computes the value of the Hamiltonian of the
4 % hierarchical three-body problem on a point.
5 % Input: a real-valued vector.
6 % Output: a real number corresponding to the value of the
7 % Hamiltonian in the point given as input.
8
9 [mi,eps,sigma,m0,mp,m,Mp,M,nCt]=constants_sigma();
10
11 H3Bs=@(z) (-1).*z(6).^(-1).*mp.*M+sigma*((1/2).*z(5).^2.*...
12 mp.^(-1)+(1/2).*z(6).^(-2).*...
13 mp.^(-1).*(-1).*z(3)+nCt).^2+(-1).*m.^2.*M.*m0.^(-1).*mi.*((-1).*z(1).*z(6)+...
14 z(1).*((1+(-1).*z(1).^(-2).*z(3).^2).^(1/2).*z(6).*cos(z(2))).^(-1).*...
15 (cos(z(4)).*((z(1).^(-2).*z(3).^2).^(1/2).*((z(3)+nCt).*cos(z(2))+z(5).*z(6).*sin(z(2)))+(z(1).^(-2).*...
16 z(3).^2).^(1/2).*z(5).*z(6).*cos(z(2))+(-1).*(z(3)+nCt).*sin(z(2))).*sin(z(4))))+eps.*...
17 ((-1/2).*z(1).^(-2).*m.^3.*M.^2+(-1).*m.*M.*mi.*((z(6).^2+z(1).^4.*m.^(-4).*...
18 M.^(-2).*(1+(-1).*(1+(-1).*z(1).^(-2).*z(3).^2).^(1/2).*cos(z(2))).^2+2.*...
19 z(1).^2.*z(6).*m.^(-2).*M.^(-1).*(((1+(-1).*z(1).^(-2).*z(3).^2).^(1/2)+...
20 cos(z(2))).*cos(z(4))+(-1).*((z(1).^(-2).*z(3).^2).^(1/2).*sin(z(2)).*sin(z(4))).^...
21 -1/2));
22
23 y=H3Bs(z0);
24
25 end

```

```

1 function dz=vector_field_sigma(t,z)
2
3 [mi,eps,sigma,m0,mp,m,Mp,M,nCt]=constants_sigma();
4
5 dz=[(-1).*((1+(-1).*(1+(-1).*z(1).^(-2).*z(3).^2).^(1/2).*cos(z(2))).^(-1).*...
6 (z(1).^(-2).*z(6).^(-1).*m.^2.*M.*m0.^(-1).*mi.*sigma.*((-1)+(1+(-1).*z(1).^(-2).*...
7 z(3).^2).^(1/2).*cos(z(2))).^(-2).*((cos(z(4)).*((1+(-1).*z(1).^(-2).*z(3).^2).^(...
8 1/2).*z(5).*z(6)+(-1).*z(5).*z(6).*cos(z(2))+z(1).^(-2).*z(3).^2).^(1/2).*((z(3)+nCt).*...
9 sin(z(2)))+((-1).*((1+(-1).*z(1).^(-2).*z(3).^2).^(1/2).*...

```

```
10 cos(z(2))+z(1).^(-2).*z(3).^2).^(1/2).*z(5).*z(6).*sin(z(2))).*sin(z(4)))+z(1).^2.*...
11 eps.*m.^(-3).*M.^(-1).*mi.*(((-1).*z(1).^2.*(1+(-1).*z(1).^(-2).*z(3).^2)).^...
12 1/2)+z(6).*m.^2.*M.*cos(z(4))).*sin(z(2))+cos(z(2)).*((z(1).^2+(-1).*z(3).^2).*sin(...))
13 z(2))+z(1).^(-2).*z(3).^2).^(1/2).*z(6).*m.^2.*M.*sin(z(4))).*(z(6).^2+z(1).^4.*m.^...
14 -4).*M.^(-2).*((-1)+(1+(-1).*z(1).^(-2).*z(3).^2).^(1/2).*cos(z(2))).^2+(-2).*...
15 z(1).^2.*z(6).*m.^(-1).*(((1+(-1).*z(1).^(-2).*z(3).^2).^(1/2)+(1+(-1).*...
16 cos(z(2))).*cos(z(4))+z(1).^(-2).*z(3).^2).^(1/2).*sin(z(2)).*sin(z(4))).^(-3/2)),...
17 (1+(-1).*((1+(-1).*z(1).^(-2).*z(3).^2).^(1/2).*cos(z(2))).^(-1).*z(6).^(-1).*...
18 m.^2.*M.*m0.^(-1).*mi.*sigma.*((-1).*z(1).^(-2).*z(1).^(-2).*z(3).^2).^(1/2)...
19 .*cos(z(2)).*(((-1)+(1+(-1).*z(1).^(-2).*z(3).^2).^(1/2).*cos(z(2))).^(-1).*((z(3)+...
20 nCt).*cos(z(4))+z(5).*z(6).*sin(z(4)))+(1+(-1).*z(1).^(-2).*z(3).^2).^(-1/2).*((1+...
21 -1).*z(1).^(-2).*z(3).^2).^(1/2)+(1+(-1).*cos(z(2))).*(z(1)+(-1).*z(1).*(1+(-1).*...
22 z(1).^(-2).*z(3).^2).^(1/2).*cos(z(2))).^(-2).*((cos(z(4)).*(z(1).^(-2).*z(3).^2).^...
23 1/2).*z(3)+nCt).*cos(z(2))+z(5).*z(6).*sin(z(2)))+(z(1).^(-2).*z(3).^2).^(1/2).*z(5).*...
24 z(6).*cos(z(2))+(1+(-1).*z(3)+nCt).*sin(z(2))).*sin(z(4)))+(-1).*z(1).^(-2).*z(3).*...
25 (1+(-1).*z(1).^(-2).*z(3).^2).^(1/2).*sin(z(2)).*(z(1).^(-1).*z(6).^(-1).*m.^2.*M.*...
26 m0.^(-1).*mi.*sigma.*((-1)+(1+(-1).*z(1).^(-2).*z(3).^2).^(1/2).*cos(z(2))).^(-...
27 -1).*((cos(z(4)).*((-1).*z(1).^(-2).*z(3).^2).^(1/2).*z(5).*z(6).*cos(z(2)))+(z(3)+nCt)...
28 .*sin(z(2)))+(z(1).^(-2).*z(3).^2).^(1/2).*z(3)+nCt).*cos(z(2))+z(5).*z(6).*sin(z(2)))...
29 .*sin(z(4)))+z(1).^2.*z(6).*eps.*m.^(-1).*mi.*((-1).*z(1).^(-2).*z(3).^2).^(1/2)...
30 .*cos(z(4)).*sin(z(2))+(1+(-1).*z(1).^(-2).*z(3).^2).^(1/2)+(1+(-1).*cos(z(2))).*...
31 sin(z(4)).*(z(6).^2+z(1).^4.*m.^(-4).*M.^(-2).*((-1)+(1+(-1).*z(1).^(-2).*...
32 z(3).^2).^(1/2).*cos(z(2))).^2+(-2).*z(1).^2.*z(6).*m.^(-2).*M.^(-1).*(((1+(-1)...
33 .*z(1).^(-2).*z(3).^2).^(1/2)+(1+(-1).*cos(z(2))).*cos(z(4))+z(1).^(-2).*z(3).^2).^(...
34 1/2).*sin(z(2)).*sin(z(4)))+(-3/2)+(-1).*eps.*z(z(1).^(-3).*m.^3.*M.^2+z(1).*(...
35 (-1).*z(1).^2+z(3).^2).^(-1).*m.^(-3).*M.^(-1).*mi.*z(6).^2+z(1).^4.*m.^(-4).*...
36 M.^(-2).*((-1)+(1+(-1).*z(1).^(-2).*z(3).^2).^(1/2).*cos(z(2))).^2+(-2).*...
37 z(1).^2.*z(6).*m.^(-2).*M.^(-1).*(((1+(-1).*z(1).^(-2).*z(3).^2).^(1/2)+(1+(-1).*...
38 cos(z(2))).*cos(z(4))+z(1).^(-2).*z(3).^2).^(1/2).*sin(z(2)).*sin(z(4))).^(-3/2).*...
39 (z(1).^2.*((4.*z(1).^2+(-3).*z(3).^2).*((1+(-1).*z(1).^(-2).*z(3).^2).^(1/2).*cos(...
40 z(2))+(-1).*((2.*z(1).^4+(-3).*z(1).^2.*z(3).^2+2.*z(3).^4).*cos(z(2)).^2+z(6).*m.^2.*M.*...
41 (2.*z(1).^2+(-1).*z(3).^2).*((1+(-1).*z(1).^(-2).*z(3).^2).^(1/2)+2.*((-1).*...
42 z(1).^2+z(3).^2).*cos(z(2))).*cos(z(4))+(-1).*z(1).^2+z(3).^2).*((2.*z(1).^2+(-1).*...
43 z(1).^(-2).*z(3).^2).^(1/2).*z(6).*m.^2.*M.*sin(z(2)).*sin(z(4))),z(1).^(-1).*...
44 z(6).^(-1).*m.^2.*M.*m0.^(-1).*mi.*sigma.*((-1)+(1+(-1).*z(1).^(-2).*z(3).^2)...).
^(-1/2).*cos(z(2))).^(-1).*((cos(z(4)).*(((-1).*z(1).^(-2).*z(3).^2).^(1/2).*z(5).*...
46 z(6).*cos(z(2))+z(3)+nCt).*sin(z(2)))+(z(1).^(-2).*z(3).^2).^(1/2).*((z(3)+nCt).*cos(...
47 z(2))+z(5).*z(6).*sin(z(2))).*sin(z(4))+z(1).^2.*z(6).*eps.*m.^(-1).*mi.*((-1).*...
48 z(1).^(-2).*z(3).^2).^(1/2).*cos(z(4)).*sin(z(2))+((1+(-1).*z(1).^(-2).*z(3).^2).^(...
49 1/2)+(-1).*cos(z(2))).*sin(z(4))).*(z(6).^2+z(1).^4.*m.^(-4).*M.^(-2).*((-1)+(1+...
50 (-1).*z(1).^(-2).*z(3).^2).^(1/2).*cos(z(2))).^2+(-2).*z(1).^2.*z(6).*m.^(-2).*...
51 M.^(-1).*(((1+(-1).*z(1).^(-2).*z(3).^2).^(1/2)+(1+(-1).*cos(z(2))).*cos(z(4))+...
52 z(1).^(-2).*z(3).^2).^(1/2).*sin(z(2)).*sin(z(4))).^(-3/2),z(6).^(-2).*mp.^(-1).*...
53 ((-1).*z(3)+nCt).*sigma+z(1).^(-3).*((z(1).^(-2).*z(3).^2).^(1/2).*z(6).^(-1).*...
54 m.^2.*M.*m0.^(-1).*mi.*sigma.*((-1)+(1+(-1).*z(1).^(-2).*z(3).^2).^(1/2).*(1/2)...
55 cos(z(2))).^(-1).*z(3).*((2.*z(3)+nCt).*cos(z(2)).*cos(z(4))+z(3).*z(5).*z(6).*...
56 cos(z(2)))+(1+(-1).*z(1).^(-2).*z(3).^2).*((1/2).*sin(z(2))).*sin(z(4))+z(1).^(-3).*z(3).*...
57 (1+(-1).*z(1).^(-2).*z(3).^2).^(1/2).*z(6).^(-1).*m.^2.*M.*m0.^(-1).*mi.*...
58 sigma.*cos(z(2)).*(((-1)+(1+(-1).*z(1).^(-2).*z(3).^2).^(1/2).*cos(z(2))).^(-2).*...
59 (cos(z(4)).*((z(1).^(-2).*z(3).^2).^(1/2).*z(3)+nCt).*cos(z(2))+z(5).*z(6).*sin(z(2)))+...
60 ((z(1).^(-2).*z(3).^2).^(1/2).*z(5).*z(6).*cos(z(2))+(-1).*z(3)+nCt).*sin(z(2))).*...
61 sin(z(4)))+(1/2).*eps.*m.*M.*mi.*z(6).^2+z(1).^4.*m.^(-4).*M.^(-2).*((-1)+(...
62 1+(-1).*z(1).^(-2).*z(3).^2).^(1/2).*cos(z(2))).^2+(-2).*z(1).^2.*z(6).*m.^(-2).*...
63 M.^(-1).*(((1+(-1).*z(1).^(-2).*z(3).^2).^(1/2)+(1/2)+(-1).*cos(z(2))).*cos(z(4))+...
64 z(1).^(-2).*z(3).^2).^(1/2).*sin(z(2)).*sin(z(4))).^(-3/2).*((2.*z(1).^2.*z(3).*m.^...
65 -4).*M.^(-2).*((1+(-1).*z(1).^(-2).*z(3).^2).^(1/2)+(-1).*cos(z(2))).*cos(z(2)))...
66 +m.^(-2).*M.^(-1).*((2.*z(3).*(1+(-1).*z(1).^(-2).*z(3).^2).^(1/2).*z(6).*cos(...
67 z(4))+(-2).*z(3).*((z(1).^(-2).*z(3).^2).^(1/2).*z(6).*sin(z(2)).*sin(z(4))))+z(1).^(-2)...
68 .*z(3).*(1+(-1).*z(1).^(-2).*z(3).^2).^(1/2).*((1+(-1).*z(1).^(-2).*z(1).^(-2).*...
69 z(3).^2).^(1/2).*cos(z(2))).^(-1).*sin(z(2)).*(((-1).*z(1).^(-2).*z(6).^(-1).*...
70 m.^2.*M.*m0.^(-1).*mi.*sigma.*((-1)+(1+(-1).*z(1).^(-2).*z(3).^2).^(1/2).*(1/2)...
71 cos(z(2))).^(-2).*((cos(z(4)).*((1+(-1).*z(1).^(-2).*z(3).^2).^(1/2).*z(5).*z(6)+(-1)...
72 .*z(5).*z(6).*cos(z(2))+z(1).^(-2).*z(3).^2).^(1/2).*z(3)+nCt).*sin(z(2)))+((-1).*...
73 1+(-1).*z(1).^(-2).*z(3).^2).^(1/2).*z(3)+nCt).*cos(z(2))+z(1).^(-2).*...
74 z(3).^2).^(1/2).*z(5).*z(6).*sin(z(2)).*sin(z(4))+(-1).*z(1).^2.*eps.*m.^(-3).*...
75 M.^(-1).*mi.*((-1).*z(1).^2.*((1+(-1).*z(1).^(-2).*z(3).^2).^(1/2)+z(6).*m.^2.*...
76 M.*cos(z(4))).*sin(z(2))+cos(z(2)).*(((z(1).^2+(-1).*z(3).^2).^(1/2).*sin(z(2))+z(1).^(-2).*...)
```

```

77 z(3).^2).^(1/2).*z(6).*m.^2.*M.*sin(z(4))).*(z(6).^2+z(1).^4.*m.^(-4).*M.^(-2).*(
78 (-1)+(1+(-1).*z(1).^(-2).*z(3).^2).^(1/2).*cos(z(2))).^2+(-2).*z(1).^2.*z(6).*m.^(
79 -2).*M.^(-1).*(((1+(-1).*z(1).^(-2).*z(3).^2).^(1/2)+(-1).*cos(z(2))).*cos(z(4))...
80 +(z(1).^(-2).*z(3).^2).^(1/2).*sin(z(2)).*sin(z(4))).^(-3/2)),z(6).^(-2).*mp.*Mp+...
81 z(1).^(-1).*z(6).^(-3).*m0.^(-1).*mp.^((-1)+(1+(-1).*z(1).^(-2).*z(3).^2)...).
82 .^(1/2).*cos(z(2))).^(-1).*((z(1).*m0.*z(3)+(-1).*nCt).^2.*sigma+(-1).*z(1).*(
83 -1).*z(1).^(-2).*z(3).^2).^(1/2).*m0.*((z(3)+(-1).*nCt).^2.*sigma.*cos(z(2))+(...).
84 z(1).^(-2).*z(3).^2).^(1/2).*z(6).*m.^2.*M.*mi.*mp.*((z(3)+nCt).*sigma.*cos(z(2)).*...
85 cos(z(4))+(-1).*z(6).*m.^2.*M.*mi.*mp.*((z(3)+nCt).*sigma.*sin(z(2)).*sin(z(4)))+(...
86 1/2).*eps.*m.*M.*mi.*((2.*z(6)+(-2).*z(1).^2.*m.^(-2).*M.^(-1).*((1+(-1).*...
87 z(1).^(-2).*z(3).^2).^(1/2)+(-1).*cos(z(2))).*cos(z(4))+z(1).^(-2).*z(3).^2).^(1/2)...
88 .*sin(z(2)).*sin(z(4))).*(z(6).^2+z(1).^4.*m.^(-4).*M.^(-2).*((-1)+(1+(-1).*...
89 z(1).^(-2).*z(3).^2).^(1/2).*cos(z(2))).^2+(-2).*z(1).^2.*z(6).*m.^(-2).*M.^(-1).*...
90 (((1+(-1).*z(1).^(-2).*z(3).^2).^(1/2)+(-1).*cos(z(2))).*cos(z(4))+z(1).^(-2).*...
91 z(3).^2).^(1/2).*sin(z(2)).*sin(z(4))).^(-3/2),(-1).*z(5).*mp.^(-1).*sigma+...
92 m.^2.*M.*mi.*sigma.*((-1).*z(1).*m0+z(1).*((1+(-1).*z(1).^(-2).*z(3).^2).^(1/2).*...
93 m0.*cos(z(2))).^(-1).*((cos(z(4)).*sin(z(2))+z(1).^(-2).*z(3).^2).^(1/2).*cos(z(2))...
94 .*sin(z(4))),z(6).^(-2).*mp.^(-1).*((z(3)+(-1).*nCt).*sigma+m.^2.*m0.^(-1).*...
95 mi.*sigma.*((-1).*z(1).*z(6)+z(1).*z(1).*(1+(-1).*z(1).^(-2).*z(3).^2).^(1/2).*z(6).*cos(...
96 z(2))).^(-1).*((z(1).^(-2).*z(3).^2).^(1/2).*cos(z(2)).*cos(z(4))+(-1).*sin(z(2)).*...
97 sin(z(4))]).';
98 end

```

A.2.2 Spatial Positions of the Bodies

In order to get the spatial position of the second and of the third body we implemented in Matlab the functions (2.12) with the choice $z = 0$ and $\iota = 0$ (which corresponds to fix $Z=C$).

```

1 function posp=xp(z0)
2
3 % This function returns the spatial position of the second
4 % body, with the choice of z=0 and i=0 (which
5 % corresponds to fix Z=C).
6 % Input: initial point of the orbit. It must be of lenght 7.
7 % Output: a 1x3 vector corresponding to the
8 % spatial position of the second body.
9
10 [mi,eps,sigma,m0,mp,m,Mp,M,nCt]=constants_sigma();
11
12 xp=@(z) [z(6).*sin(z(7)),(-1).*z(6).*cos(z(7)),0];
13
14 posp=xp(z0);
15
16 end

```

```

1 function pos=x(z0)
2
3 % This function returns the spatial position of the third
4 % body, with the choice of z=0 and i=0 (which
5 % corresponds to fix Z=C).
6 % Input: initial point of the orbit. It must be of lenght 7.
7 % Output: a 1x3 vector corresponding to the
8 % spatial position of the third body.
9
10
11 [mi,eps,sigma,m0,mp,m,Mp,M,nCt]=constants_sigma();
12 x=@(z) ...
13     [z(1).^2.*m.^(-2).*M.^(-1).*((( -1).* (1+(-1).*z(1).^(-2).*z(3).^2)...
14     .^(1/2)+cos(z(2))).*(cos(z(7)).*sin(z(4))+(-1).*cos(z(4)).*sin(z(7)))...
15     +(z(1).^(-2).*z(3).^2).^ (1/2).*sin(z(2)).*(cos(z(4)).*cos(z(7))...
16     +sin(z(4)).*sin(z(7))));z(1).^2.*m.^(-2).*M.^(-1).*((z(1).^(-2).*z(3)...
17     .^2).^(1/2).*sin(z(2)).*(( -1).*cos(z(7)).*sin(z(4))+cos(z(4)).*...
18     sin(z(7)))+((-1).* (1+(-1).*z(1).^(-2).*z(3).^2).^(1/2)+cos(z(2))).*...
19     (cos(z(4)).*cos(z(7))+sin(z(4)).*sin(z(7)))));0];
20 pos=x(z0);
21
22 end

```

A.2.3 Numerical Solution of the Hamiltonian ODEs

For the actual numerical solutions of the Hamiltonian ODEs we used the following Matlab code. The ode solver `ode23s` has been chosen because for particular initial values the differential equations are stiff.

```

1 function [z,t]=sol_sigma(z0,Ti,Tf)
2
3 % This function provides and approximation of the flux of the
4 % Hamiltonian vector field with initial point z0 on the time
5 % interval [Ti,Tf].
6 %
7 % Input
8 % z0: initial value, it must be a row vector.

```

```

9 % Ti: it represents the approximation of the solution
10 % backward in time, so it must be a negative real number.
11 % Tf: the final time of approximation
12
13 opts = odeset('Refine',6);
14 [s,u] = ode23s(@vector_field_sigma, [0 Ti], z0,opts);
15 [tau,v] = ode23s(@vector_field_sigma, [0 Tf], z0,opts);
16 % the angles are 2-pi periodic
17 u(:,2)=mod(u(:,2),2*pi);
18 u(:,4)=mod(u(:,4),2*pi);
19 u(:,6)=mod(u(:,6),2*pi);
20 v(:,2)=mod(v(:,2),2*pi);
21 v(:,4)=mod(v(:,4),2*pi);
22 v(:,6)=mod(v(:,6),2*pi);
23
24 % the solution
25 z=vertcat(flip(u),v);
26 t=vertcat(flip(s),tau);
27
28 end

```

Then we used the following code for the analysis of a single orbit.

```

1 clear
2 close all
3 format shorte
4 [mi,eps,sigma,m0,mp,m,Mp,M,nCt]=constants_sigma();
5 % case delta=0.5
6 L=sqrt(2);
7 G=.4;
8 a0=L^2/(M*m^2);
9 r=eps^2.*((nCt-G).^2./(Mp.*mp.^2));
10
11
12 %% The Solution
13 z0=[L 3. G 1. 0 r 2.];
14 %z0=[L 3 .5 3. 1e-6 100];
15 [z,t]=sol_sigma(z0,-3e10,3e10);
16

```

```

17 pos=zeros(3,length(z));
18 posprimo=zeros(3,length(z));
19
20 for i=1:length(z)
21     pos(:,i)=x(z(i,:));
22     posprimo(:,i)=xp(z(i,:));
23 end
24
25
26 %% Spatial Configuration
27 figure
28 hold on
29 % yellow circle in the origin for the first body
30 th = 0:pi/50:2*pi;
31 xunit = .02 * cos(th);
32 yunit = .02 * sin(th);
33 zunit= zeros(1,101);
34 fill3(xunit, yunit,zunit,'Yellow');
35 % second body
36 plot3(posprimo(1,:),posprimo(2,:),posprimo(3,:),'b.','MarkerSize',1)
37 plot3(pos(1,:),pos(2,:),pos(3,:),'r.','MarkerSize',1)
38 daspect([1 1 1])
39 legend('I body', 'II body', 'III body')
40 hold off
41
42
43 %% The various plots
44 figure('rend','painters','pos',[250 100 1100 500])
45 % L
46 subplot(2,6,1)
47 plot(t,z(:,1),'.','MarkerSize',2,'Color','Black')
48 xlabel('time')
49 ylabel('L')
50 ylim([-L-.5 L+.5])
51 title('L')
52 % l
53 subplot(2,6,2)
54 plot(t,z(:,2)-sqrt(1-z(:,3).^2./z(:,1).^2).*sin(z(:,2))...
55     ,'.','MarkerSize',2,'Color','Black')

```

```
56 xlabel('time')
57 ylabel('l')
58 title('l')
59 % G
60 subplot(2,6,3)
61 plot(t,z(:,3),'.','MarkerSize',2,'Color','Black')
62 xlabel('time')
63 ylabel('G')
64 %ylim([-L L])
65 title('G')
66 % g
67 subplot(2,6,4)
68 plot(t,z(:,4),'.','MarkerSize',2,'Color','Black')
69 xlabel('time')
70 ylabel('g')
71 title('g')
72 % R
73 subplot(2,6,5)
74 plot(t,z(:,5),'.','MarkerSize',2,'Color','Black')
75 xlabel('time')
76 ylabel('R')
77 title('R')
78 %ylim([-1,1])
79 %r
80 subplot(2,6,6)
81 plot(t,z(:,6),'.','MarkerSize',2,'Color','Black')
82 xlabel('time')
83 ylabel('r')
84 title('r')
85 %ylim([0,2])
86 % L-l
87 subplot(2,6,[7 8])
88 plot(z(:,1),z(:,2)-sqrt(1-z(:,3).^2./z(:,1).^2).*sin(z(:,2))...
89     ,'.','MarkerSize',2,'Color','Black')
90 title('L-l')
91 xlabel('L')
92 ylabel('l')
93 xlim([L-.5 L+.5])
94 % g-G
```

```

95 subplot(2,6,[9 10])
96 plot(z(:,4),z(:,3),'.', 'MarkerSize',2,'Color','Black')
97 title('g-G')
98 xlabel('g')
99 ylabel('G')
100 xlim([0 2*pi])
101 ylim([-L L])
102 % R-r
103 subplot(2,6,[11 12])
104 plot(z(:,5),z(:,6),'.', 'MarkerSize',2,'Color','Black')
105 title('R-r')
106 xlabel('R')
107 ylabel('r')
108 %xlim([-2 2])
109 %ylim([.5 1.5])
110
111 %% Conservation of Energy along an orbit
112 v0=ones(1,length(z)).*H3Bs(z0);
113 v=zeros(1,length(z));
114 for i=1:length(z)
115     v(i)=H3Bs(z(i,:));
116 end
117 err=norm(v0-v);
118
119 delta0=z0(6)/a0; % the initial value
120 % of delta
121
122 fprintf('\n ERRORE: %3e \n DELTA: %3f \n',err,delta0)

```

A.3 Phase Portraits

In order to get the phase portraits reported in this thesis we used the the following codes.

The function with which we declared the value of the constants is the following.

```

1 function ...
    [mi,eps,sigma,m0,mp,m,Mp,M,nCt]=constants_phaseportrait()

```

```

2      mi = 1E-2; eps = 1E-7;
3      m0 = 1;
4      mp = m0/(1+mi);
5      m = m0/(1 + mi*eps);
6      Mp=m0*(1+mi);
7      M = m0*(1+eps*mi);
8      sigma=0;
9      nCt=eps^(-1);
10 end

```

We modified the values of the parameters mi , eps and $sigma$ in this function according to our various attempts.

Next is reported the code used to draw the phase portrait for the two centre problem for $\delta = 0.505$ and for $\delta = 1.515$.

```

1 % This Script gives a phase portrait in the plane g-G
2 % for the two centre problem. Varing the parameter sigma
3 % and accordingly the integration times yields to the
4 % phase portrait for the hierarchical three.body problem.
5
6 clear
7 close all
8 format shorte
9
10 %% Constants
11 [mi,eps,sigma,m0,mp,m,Mp,M,nCt]=constants_phaseportrait();
12
13 % case delta=0.505
14 L=sqrt(2);
15 a0=L^2/(M*m^2);
16
17
18 %% The Phase Portrait
19 figure
20
21 hold on
22
23 G=.1;
24 r=eps^2.*((nCt-G).^2./(Mp.*mp.^2));
25 z0=[L 3. G 3. 0 r 2.];

```

```

26 [z,~]=sol_sigma_phaseportr(z0,-4e10,1.6e10);
27 plot(z(:,4),z(:,3),'.', 'MarkerSize',2)
28
29 G=.3;
30 r=eps^2.*((nCt-G).^2./(Mp.*mp.^2));
31 z0=[L 3. G 3. 0 r 2.];
32 [z,~]=sol_sigma_phaseportr(z0,-5e10,5e10);
33 plot(z(:,4),z(:,3),'.', 'MarkerSize',2,'Color','Black')
34
35 G=.5;
36 r=eps^2.*((nCt-G).^2./(Mp.*mp.^2));
37 z0=[L 3. G 3. 0 r 2.];
38 [z,~]=sol_sigma_phaseportr(z0,-4.3e10,2.5e10);
39 plot(z(:,4),z(:,3),'.', 'MarkerSize',2,'Color','Black')
40
41 G=.7;
42 r=eps^2.*((nCt-G).^2./(Mp.*mp.^2));
43 z0=[L 3. G 3. 0 r 2.];
44 [z,~]=sol_sigma_phaseportr(z0,-4.3e10,2.5e10);
45 plot(z(:,4),z(:,3),'.', 'MarkerSize',2,'Color','Black')
46
47 G=.9;
48 r=eps^2.*((nCt-G).^2./(Mp.*mp.^2));
49 z0=[L 3. G 3. 0 r 2.];
50 [z,~]=sol_sigma_phaseportr(z0,-3.5e10,8e9);
51 plot(z(:,4),z(:,3),'.', 'MarkerSize',2,'Color','Black')
52
53 G=1.1;
54 r=eps^2.*((nCt-G).^2./(Mp.*mp.^2));
55 z0=[L 3. G 3. 0 r 2.];
56 [z,~]=sol_sigma_phaseportr(z0,-1.35e10,8e9);
57 plot(z(:,4),z(:,3),'.', 'MarkerSize',2,'Color','Black')
58
59 G=1.3;
60 r=eps^2.*((nCt-G).^2./(Mp.*mp.^2));
61 z0=[L 3. G 3. 0 r 2.];
62 [z,~]=sol_sigma_phaseportr(z0,-1.35e10,8e9);
63 plot(z(:,4),z(:,3),'.', 'MarkerSize',2,'Color','Black')
64

```

```

65 G=-1.3;
66 r=eps^2.*((nCt-G).^2./(Mp.*mp.^2));
67 z0=[L 3. G 3. 0 r 2.];
68 [z,t]=sol_sigma_phaseportr(z0,-4e10,1e10);
69 plot(z(:,4),z(:,3),'.','MarkerSize',2,'Color','Black')
70
71 G=-L+.1;
72 r=eps^2.*((nCt-G).^2./(Mp.*mp.^2));
73 z0=[L 3. G 3. 0 r 2.];
74 [z,t]=sol_sigma_phaseportr(z0,-1e10,1e10);
75 plot(z(:,4),z(:,3),'.','MarkerSize',2,'Color','Black')
76
77 axis([0 2*pi -L L])

```

```

1 % This Script gives a phase portrait in the plane g-G
2 % for the two centre problem. Varing the parameter sigma
3 % and accordingly the integration times yields to the
4 % phase portrait for the hierarchical three.body problem.
5
6 clear
7 close all
8 format shorte
9
10 %% Constants
11 [mi,eps,sigma,m0,mp,m,Mp,M,nCt]=constants_sigma_two_centre();
12 % case delta=1.515
13 L=sqrt(2)/sqrt(3);
14 a0=L^2/(M*m^2);
15
16
17 %% The Phase Portrait
18 f1=figure;
19 hold on
20
21 G=.1;
22 r=eps^2.*((nCt-G).^2./(Mp.*mp.^2));
23 z0=[L 3. G 3. 0 r 2.];
24 [z,~]=sol_sigma_two_centre(z0,-3e10,1.6e10);

```

```

25 plot(z(:,4),z(:,3),'.', 'MarkerSize',2,'Color','Black')
26
27 G=.3;
28 r=eps^2.*((nCt-G).^2./(Mp.*mp.^2));
29 z0=[L 3. G 3. 0 r 2.];
30 [z,~]=sol_sigma_two_centre(z0,-2e10,1.5e10);
31 plot(z(:,4),z(:,3),'.', 'MarkerSize',2,'Color','Black')
32
33 G=.7;
34 r=eps^2.*((nCt-G).^2./(Mp.*mp.^2));
35 z0=[L 3. G 3. 0 r 2.];
36 [z,~]=sol_sigma_two_centre(z0,-6e9,7.5e9);
37 plot(z(:,4),z(:,3),'.', 'MarkerSize',2,'Color','Black')
38
39 G=.8;
40 r=eps^2.*((nCt-G).^2./(Mp.*mp.^2));
41 z0=[L 3. G 3. 0 r 2.];
42 [z,~]=sol_sigma_two_centre(z0,-2.61e9,4.5e9);
43 plot(z(:,4),z(:,3),'.', 'MarkerSize',2,'Color','Black')
44
45 G=.45;
46 r=eps^2.*((nCt-G).^2./(Mp.*mp.^2));
47 z0=[L 3. G .05 0 r 2.];
48 [z,~]=sol_sigma_two_centre(z0,-1e9,1e9);
49 plot(z(:,4),z(:,3),'.', 'MarkerSize',2,'Color','Black')
50
51 G=-.45;
52 r=eps^2.*((nCt-G).^2./(Mp.*mp.^2));
53 z0=[L 3. G .05 0 r 2.];
54 [z,~]=sol_sigma_two_centre(z0,-1e9,1e9);
55 plot(z(:,4),z(:,3),'.', 'MarkerSize',2,'Color','Black')
56
57 G=.6;
58 r=eps^2.*((nCt-G).^2./(Mp.*mp.^2));
59 z0=[L 3. G .05 0 r 2.];
60 [z,~]=sol_sigma_two_centre(z0,-5e7,5e7);
61 plot(z(:,4),z(:,3),'.', 'MarkerSize',2,'Color','Black')
62
63 G=-.6;

```

```
64 r=eps^2.*((nCt-G).^2./(Mp.*mp.^2));
65 z0=[L 3. G .05 0 r 2.];
66 [z,~]=sol_sigma_two_centre(z0,-5e7,5e7);
67 plot(z(:,4),z(:,3),'.', 'MarkerSize',2,'Color','Black')
68
69 G=.5;
70 r=eps^2.*((nCt-G).^2./(Mp.*mp.^2));
71 z0=[L 3. G 2.8 0 r 2.];
72 [z,~]=sol_sigma_two_centre(z0,-6.2e9,1.6e10);
73 plot(z(:,4),z(:,3),'.', 'MarkerSize',2,'Color','Black')
74
75 axis([0 2*pi -L L])
```


Bibliography

- [1] V. I. Arnol'd. Proof of a theorem of A. N. Kolmogorov on the preservation of conditionally periodic motions under a small perturbation of the Hamiltonian. *Uspehi Mat. Nauk*, 18(5 (113)):13–40, 1963.
- [2] A. A. Bekov and T. B. Oмаров. Integrable cases of the Hamilton-Jacobi equation and some nonsteady problems of celestial mechanics. *Soviet Astronomy*, 22:366–370, May-June 1978.
- [3] G. Benettin. The Elements of Hamiltonian Perturbation Theory, 2005.
- [4] F. Biscani and D. Izzo. A complete and explicit solution to the three-dimensional problem of two fixed centres, [ArXiv: 1510.07959]. 455:3480–3493, February 2016.
- [5] C. Charlier *Die Mechanik des Himmels*. Vorlesungen, 1907.
- [6] L. Euler. De motu corporis ad duo centra virium fixa attracti. *Novi Commentarii Academiae Scientiarum Imperialis Petropolitanae*, Tome X (1764/65) p. 207; Tome XI (1765/67) p. 152.
- [7] L. Euler. Un corps étant attiré en raison réciproque quarrée des distances vers deux points fixes donnés. *Mémoires de Berlin*, page 28, 1760.
- [8] F. Fassò. Lie series method for vector fields and Hamiltonian perturbation theory. *Z. Angew. Math. Phys.*, 41(6):843–864, 1990.
- [9] F. Fassò. Hamiltonian perturbation theory on a manifold. *Celestial Mech. Dynam. Astronom.*, 62(1):43–69, 1995.
- [10] F. Fassò. Superintegrable Hamiltonian systems: geometry and perturbations. *Acta Appl. Math.*, 87(1-3):93–121, 2005.
- [11] C. G. J. Jacobi. *Jacobi's lectures on dynamics*, volume 51 of *Texts and Readings in Mathematics*. Hindustan Book Agency, New Delhi,

- revised edition, 2009. Delivered at the University of Königsberg in the winter semester 1842–1843 and according to the notes prepared by C. W. Brockardt, Edited by A. Clebsch, Translated from the original German by K. Balagangadharan, Translation edited by Biswarup Banerjee.
- [12] A. N. Kolmogorov. On conservation of conditionally periodic motions for a small change in Hamilton's function. *Dokl. Akad. Nauk SSSR (N.S.)*, 98:527–530, 1954.
 - [13] A. Morbidelli. *Modern Celestial Mechanics: Dynamics in the Solar System*. Taylor & Francis, 2002.
 - [14] J. Moser. On invariant curves of area-preserving mappings of an annulus. *Nachr. Akad. Wiss. Göttingen Math.-Phys. Kl. II*, 1962:1–20, 1962.
 - [15] N. N. Nehoroshev. An exponential estimate of the time of stability of nearly integrable Hamiltonian systems. *Uspehi Mat. Nauk*, 32(6(198)):5–66, 287, 1977.
 - [16] I. Newton. *Philosophiae naturalis principia mathematica*. J. Societatis Regiae ac Typis J. Streater, 1687.
 - [17] D. Ó Mathúna. *Integrable systems in celestial mechanics*, volume 51 of *Progress in Mathematical Physics*. Birkhäuser Boston, Inc., Boston, MA, 2008. With an appendix by Vincent G. Hart and Seán Murray.
 - [18] G. Pinzari. Aspects of the planetary Birkhoff normal form. *Regul. Chaotic Dyn.*, 18(6):860–906, 2013.
 - [19] G. Pinzari. An analysis of the Sun-Earth-Asteroid systems based on the two-centre problem, [ArXiv:1702.03680]. February 2017.
 - [20] G. Pinzari. Work in progress, private communication. 2018.
 - [21] H. Poincaré. *Les Methodes Nouvelles de la Mecanique Celeste*. Gauthier-Villars et fils Paris, 1892.
 - [22] H. R. Dullin and R. Montgomery. Syzygies in the two center problem. *Nonlinearity*, 29(4):1212–1237, 2016.
 - [23] H. R. Waalkens, H. Dullin and P. H. Richter. The problem of two fixed centers: bifurcations, actions, monodromy. *Phys. D*, 196(3-4):265–310, 2004.